Quantum circuit approximations and entanglement renormalization for the Dirac field in 1+1 dimensions

Freek Witteveen[1], Volkher Scholz[2], Brian Swingle[3], and Michael Walter[1,4]

[1]Korteweg-de Vries Institute for Mathematics and QuSoft, University of Amsterdam
[2]Department of Physics, Ghent University
[3]Condensed Matter Theory Center, Maryland Center for Fundamental Physics, Joint Center for Quantum Information and Computer Science, and Department of Physics, University of Maryland
[4]Institute for Theoretical Physics, Institute for Language, Logic, and Computation, University of Amsterdam

Abstract

The multiscale entanglement renormalization ansatz describes quantum many-body states by a hierarchical entanglement structure organized by length scale. Numerically, it has been demonstrated to capture critical lattice models and the data of the corresponding conformal field theories with high accuracy. However, a rigorous understanding of its success and precise relation to the continuum is still lacking. To address this challenge, we provide an explicit construction of entanglement-renormalization quantum circuits that rigorously approximate correlation functions of the massless Dirac conformal field theory. We directly target the continuum theory: discreteness is introduced by our choice of how to probe the system, not by any underlying short-distance lattice regulator. To achieve this, we use multiresolution analysis from wavelet theory to obtain an approximation scheme and to implement entanglement renormalization in a natural way. This could be a starting point for constructing quantum circuit approximations for more general conformal field theories.

Contents

1 Introduction

Quantum information theory is generally formulated in terms of discrete quantum bits and quantum circuits. However, our most fundamental theories of nature are formulated as quantum field theories, and it is a physical and mathematical challenge to understand the role of quantum information in such continuum theories. In this work, we bridge these two paradigms for the case of a free massless Dirac field in 1+1 dimensions and show how to rigorously represent its entanglement structure through a quantum circuit.

Quantum circuits are examples of tensor networks, which parameterize quantum many-body states with a relatively small number of parameters by restricting the allowed entanglement structure. Tensor networks have been very successful for studying discrete quantum systems [1]. Several approaches have been proposed to extend the notion of a quantum circuit, or more generally of a tensor network, to quantum field theories. Roughly speaking there are two distinct routes: one is to define a variational class of continuum states, whereas the other is to consider a restricted set of observables and try to approximate correlation functions of these observables.

An example of the former is cMERA [2], which defines a class of states that arise from a real-space renormalization procedure. In this case the 'quantum circuit' that performs the entanglement renormalization is also continuous. Another example is cMPS [3], which can be interpreted as a path integral [4]. Both approaches have been successfully demonstrated numerically for free theories, and these classes of states have also been used as a basis for perturbation theory [5] and variational algorithms [6] for 1+1 dimensional quantum field theories.

In this paper, we follow the second route, by considering correlation functions of smeared operators. These operators are discretized at an appropriate scale and an ordinary quantum circuit

circuit is used to prepare a state with which to compute their correlation functions. This means that the discreteness in our description arises not from the system itself, but in our choice of how to probe the system.

The circuits that we derive fit in the Multi-scale Entanglement Renormalization Ansatz (MERA) [8, 9], a tensor network ansatz designed for systems with scale invariance that implements a kind of real-space renormalization. A MERA tensor network prepares a quantum many-body state through a series of layers, each of which consists of isometries followed by local unitary transformations. If we apply the circuit in reverse, the latter disentangle local degrees of freedom and the former coarse-grain the system by a factor of two. For a scale-invariant theory, each of these layers can be taken identical, and it has been demonstrated numerically for some paradigmatic Hamiltonians that the conformal data of the limiting theory, such as the scaling dimensions and operator product expansion (OPE) coefficients, can be extracted from the scaling superoperator corresponding to a single network layer [10].

Tensor networks have to a large extent been developed as a method to efficiently simulate quantum systems on a classical computer. However, evaluating correlation functions for a MERA tensor network can still be very costly, with the computational cost scaling as a high power of the number of parameters. If one extends the MERA to a quantum circuit, it can be simulated efficiently on a quantum computer provided the complexity of each layer is not too large. It has been argued that the structure of entanglement renormalization may be relatively insensitive to small errors and that many models of physical interest have layers of low complexity, thus it may be a useful circuit model for quantum computers to simulate quantum systems at or away from criticality [11]. In this regard, our results provide additional evidence that tensor networks are a promising application of noisy quantum computers, as we now also have the possibility to address continuum theories.

A final motivation to investigate tensor networks for conformal field theories is provided by the wish to study holography (a duality between two quantum theories, one in d dimensions and one in $d+1$ dimensions). The main example is provided by the AdS/CFT correspondence, a conjectural relation between quantum gravity on an AdS space with a conformal field theory on its conformal boundary [15]. It has been remarked that entanglement renormalization has a structure reminiscent of this duality [16], as the circuit reorganizes a critical one-dimensional system to a two-dimensional structure that is a discretization of AdS space, although the precise connection to holographic theories is still being developed [17, 18]. Any MERA tensor network can be extended to a unitary quantum circuit by extending the isometries to unitaries with an auxiliary input, so that the MERA is recovered by applying the circuit to an appropriate product state. Such extensions are not unique. In contrast, our construction naturally yields a unitary quantum circuit that reorganizes the degrees of freedom of the Dirac theory in one higher dimension, by position and scale, cleanly separating positive and negative energy modes of the Dirac fermion. Thus it can be seen as a circuit realization of a holographic mapping for an actual conformal field theory, complementing tensor network toy models of holographic mappings as proposed in [19–22].

1.1 Prior work

1.2 Summary of results

We now describe our main results. The model that we consider is the free massless Dirac fermion in 1+1 dimensions, with action

$$S(\Psi) = \frac{1}{2}\int \Psi^\dagger \gamma^0 \gamma^\mu \partial_\mu \Psi \, dx dt$$

for a two-component complex fermionic field Ψ on the line (or on a circle). The usual second quantization procedure shows that the fields have correlation function

$$\langle \Psi^\dagger(x)\Psi(y)\rangle = \frac{1}{x-y}.$$

The stress energy tensor is a normal-ordered product of the fields and its derivatives. In complex coordinates $z = x + it$ and $\bar{z} = x - it$, the stress-energy tensor has a holomorphic T_{zz} component for which one may deduce that

$$\langle T_{zz}(x)T_{zz}(y)\rangle = \frac{1/2}{(x-y)^4}$$

and hence the theory has central charge $c = 1$. For details from the conformal field theory point of view, see [28]. We will briefly review the algebraic approach to the Dirac fermion in Section 2. In this approach, in order to have well-behaved operators, one usually 'smears' the fields. That is, for some function f one defines

$$\Psi(f) = \int f(x)\Psi(x)dx.$$

From a physical perspective the smearing function is justified by the fact that one can only probe the system at some finite scale.

We will now describe a procedure which approximates correlation functions of smeared operators. Informally, the procedure is that we first discretize the operators at some scale (i.e., we impose a UV cut-off), and then, in order to obtain the free fermion vacuum, we need to 'fill the Dirac sea' up to the relevant scale. So, the circuit, starting from the Fock vacuum, has to fill all the negative energy modes over the range of scales that are relevant for the inserted operators, directly analogous to a real-space renormalization procedure. We know the negative energy states explicitly in Fourier space, but the non-trivial problem is that we want to construct a *local* circuit, while the Fourier basis for the negative energy solutions is very non-local. In order to obtain a circuit that is compatible with scale invariance and translation invariance, but is still local, we are led to search for a *wavelet* basis for the space of negative energy solutions. It is not possible to construct a basis that is both completely local and consists of exactly negative energy solutions, but it turns out it is approximately possible by using a pair of wavelets that approximately satisfy a certain phase relation. Such pairs of wavelets, called *approximate Hilbert pairs* have already been constructed for other purposes [29], and as discussed in Section 1.1 these are closely related to the construction of (approximate) ground states for critical free fermions. This construction takes as input two integer parameters K and L, such that the support of the wavelet is of size $2(K + L)$, and there is an approximation parameter ε which measures how accurately the phase relation is satisfied.

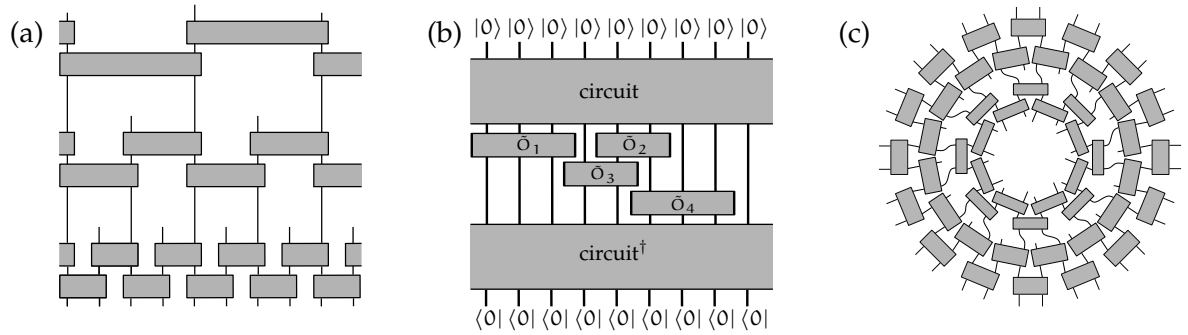

Figure 1: (a) Structure of the circuit for the Dirac fermion on the line. Each layer is an identical local quantum circuit of depth $K + L$. (b) Correlation functions (1.1) are computed as expectation values of discretizations $\tilde{O}_i$ of the operators O_i. (c) Periodized circuit for the Dirac fermion on the circle.

The wavelet functions give rise to a 'classical' circuit, which implements the decomposition of a function in the wavelet basis at different scales. This circuit should be thought of as a circuit on the single-particle level, and the fermionic quantum circuit is obtained as its second quantization.

Now let $\{O_i\}$, $i = 1, \ldots, n$ be a set of smeared operators that are either linear in the fields or normal-ordered quadratic operators, and which are compactly supported. We denote the correlation functions by

$$G(\{O_i\}) = \langle O_1 \cdots O_n \rangle. \tag{1.1}$$

The procedure sketched above discretizes the operators O_i and constructs a quantum circuit that computes an approximation $G^{\mathrm{MERA}}_{\mathcal{L},\varepsilon}(\{O_i\})$ of the correlation function, where $\mathcal{L}$ is the number of layers of the circuit, and ε is an error parameter. The structure of the circuit is illustrated in Fig. 1 (both for the line and circle).

The following is a simplified version of our main result. A precise formulation is given by Theorem 4.5, where we also specify precisely which operators we consider and give explicit bounds for the approximation error. We assume that we are given a family of wavelet filters with uniformly bounded scaling functions, of support M and approximating the Hilbert pair relation to accuracy ε. The constructed circuits have depth $D = \lceil \frac{M}{2} \rceil$ for a single circuit layer, and the bond dimension of the corresponding MERA tensor network is given by $\chi = 2^D$.

Theorem 1.1 (Informal)**.** *Let $O_1, \ldots, O_n$ be a collection of Dirac field creation or annihilation operators or normal-ordered quadratic operators with compact support and smeared by a differentiable function. Then the approximation error is bounded by*

$$|G(\{O_i\}) - G^{\mathrm{MERA}}_{\mathcal{L},\varepsilon}(\{O_i\}| = \mathcal{O}(M^2 2^{-\frac{\mathcal{L}}{3}}) + \mathcal{O}(\varepsilon \log \tfrac{M}{\varepsilon}).$$

The constants in the $\mathcal{O}$-notation depend on n and the support and smoothness of the O_i.

Our main theorem provides a justification for the numerical success of MERA for quantum field theories by providing rigorous bounds on the approximation of correlation functions. To illustrate our result, we show the precise error bounds obtained for a two-point function in Fig. 2. The error bounds in Theorem 1.1 are invariant under rescaling (which is of course a desirable property for a scale invariant theory). A Dirac fermion can be decomposed into two Majorana fermions.

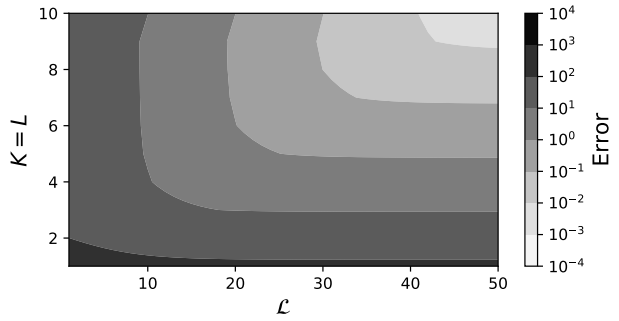

Figure 2: The error bound from Theorem 1.1 (Theorem 4.5) illustrated for a two-point function. It is obtained by evaluating Eq. (4.11) using Table 2 for an approximate Hilbert pair with parameters $K = L$. The smearing functions are taken to be translates of a function f with $\|f\| = 1$ and optimal trade-off between smoothness and support (that is, $D = \sqrt{2}$ in the formulation of Theorem 4.5).

Our construction is compatible with this decomposition, so we also obtain quantum circuits for Majorana fermions.

Note that our construction gives rise to a circuit rather than a MERA tensor network in a canonical way, and that the bond dimension is exponential in the circuit depth, so this provides a potential starting point for investigating quantum algorithms for quantum field theory correlation functions. One of the interesting features of 1+1 dimensional conformal field theories is that they have many symmetries. Discretizing the theory necessarily breaks these symmetries. However, we find that spatial translation, time translation and rescaling by a factor two all have natural implementations on the MERA (where rescaling by a factor 2 is precisely implemented by a single circuit layer).

Numerical examples

Since the circuits we obtain are the second quantization of a single-particle circuit we can simulate them for high circuit depth (bond dimension). In Fig. 3, (a) and (b) we show approximations to the smeared two-point functions for the fermionic fields and for the stress-energy tensor for $K = L = 1$ and $K = L = 3$ in the wavelet construction, corresponding to MERA tensor networks with bond dimensions $\chi = 4$ and $\chi = 64$ respectively. Another statistic is the entanglement entropy of an interval. In order to define this one needs a cut-off, for which we use the wavelet discretization. The Cardy formula [35] predicts that for a conformal field theory the entanglement entropy of an interval scales as $S_E = \frac{c}{3}\log(L) + c'$ where c is the central charge, L is the size of the interval, and c' a non-universal constant depending on the cut-off. In Fig. 3, (c) we have plotted the entanglement entropies obtained from our construction (for the same wavelets). For $K = L = 3$ the agreement with the Cardy formula for $c = 1$ is already very accurate. As another numerical illustration of the accuracy of approximation, one may compute eigenvalues of the entanglement renormalization superoperator and extract scaling dimensions of the conformal field theory from its eigenvalues [36]. One way to do so is by applying a Jordan-Wigner transformation to the circuit for the Majorana fermion to obtain a (matchgate) circuit for the Ising model, following the procedure in [12]. The results are illustrated in Table 1.

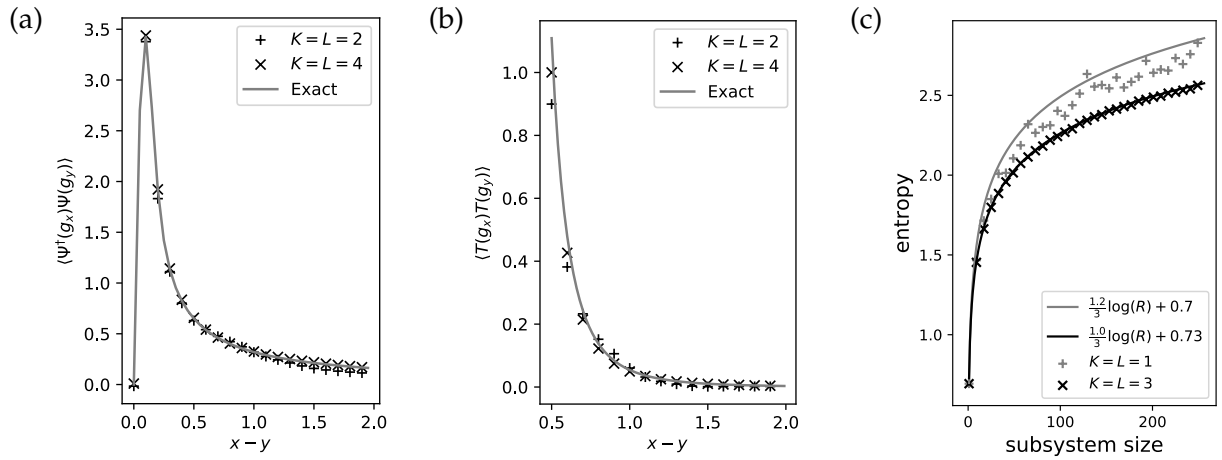

Figure 3: (a) Correlation function $\langle \Psi^\dagger(g_x)\Psi(g_y)\rangle$ evaluated using our approximate quantum circuits. The smearing functions g_x, g_y are Gaussians with standard deviation $\sigma = 0.05$ peaked at x and y, respectively. (b) Correlation functions $\langle T(g_x)T(g_y)\rangle$ evaluated using our approximation quantum circuits. The stress-energy tensor is smeared in both space and time; see Section 4.2 for details. (c) Subsystem entropies for the corresponding quantum states. The logarithmic fits show that we obtain excellent agreement with the Cardy formula for central charge $c = 1$ already for $K + L = 6$.

	χ	E	$\Delta E/E$	Δ_σ	Δ_μ
Exact		$-\frac{4}{\pi}$		0.125	0.125
$K = 1, L = 1$	2	-1.2560	0.0135	0.0968	0.1696
$K = 1, L = 2$	4	-1.2705	0.0021	0.1360	0.1173
$K = 2, L = 1$	4	-1.2630	0.0081	0.1031	0.1563
$K = 1, L = 3$	8	-1.2727	0.0005	0.1226	0.1283
$K = 2, L = 2$	8	-1.2722	0.0008	0.1310	0.1204
$K = 3, L = 1$	8	-1.2655	0.0061	0.1052	0.1522
$K = 1, L = 4$	16	-1.2731	0.0001	0.1261	0.1242
$K = 2, L = 3$	16	-1.2731	0.0001	0.1238	0.1264

Table 1: Values of the Majorana fermion energy density E, the relative error in energy density $(E + \frac{\pi}{2})/E$ and the scaling dimensions Δ_σ and Δ_μ for the Majorana CFT (or, equivalently, of the Ising CFT). Some other scaling dimensions, in particular those of the fermion fields themselves, are exactly reproduced because of the structure of the wavelet transform, as discussed in Section 5.4. These values were computed by first decoupling the circuit obtained from an approximate Hilbert pair of wavelets for the Dirac fermion into two circuits for Majorana fermions, and then taking a Jordan-Wigner transform. This yields an entanglement renormalization circuit for the Ising model, in which the spin and disorder fields σ and μ are local. For details on this procedure, see [12].

1.3 Outlook

As mentioned, our quantum circuits implement a 'holographic mapping' for the Dirac conformal field theory. This opens up the possibility to study many interesting questions on how quantum information is organized by such mappings, e.g., in terms of quantum error correcting properties [37].

In future work we hope to construct entanglement renormalization circuits for more general classes of conformal field theories. A challenging open problem is to extend the relation between wavelet analysis and quantum circuits for conformal field theories to interacting models. It is not at all clear that this is possible, but a natural starting point could be Wess-Zumino-Witten theories, as many of these can be constructed algebraically as symmetries on a finite number of free massless fermions [38].

Another direction would be to investigate entanglement renormalization from the perspective of vertex algebras. A recent attempt to discretize vertex algebras to a spin chain model, with a view towards quantum computer simulation of conformal field theories can be found in [40].

From a computational point of view it would be interesting to investigate whether a wavelet circuit can serve as a starting point for perturbation theory, and get faster convergence of MERA optimization algorithms.

1.4 Plan of the paper

The remainder of this work is structured as follows: in Section 2 we recall the algebraic approach to fermionic systems and quasi-free states, in Section 3 we review wavelet theory and collect some useful estimates. Section 4 contains the main results, first we derive a wavelet approximation to the free fermion, then use it to construct a quantum circuit and we prove a bound on the approximation error. We also discuss how to implement certain conformal symmetries with the circuit and remark on the possibility of reproducing conformal data.

1.5 Notation and conventions

Given a Hilbert space $\mathbb{H}$, we write $\langle \cdot, \cdot \rangle$ for the inner product and $\|\cdot\|$ for the norm of vectors. We denote by $B(\mathbb{H})$ the space of bounded operators on $\mathbb{H}$ and the operator norm of an operator A by $\|A\|$. We denote Hermitian adjoints by $A^\dagger$, and we write $A \leqslant A'$ if the difference $A' - A$ is positive semidefinite. We denote identity operators by $\mathbb{1}_{\mathbb{H}}$ and leave out the subscript if the Hilbert space is clear from the context. If A is Hilbert-Schmidt then we write $\|A\|_2 = \sqrt{\mathrm{tr}[A^\dagger A]}$ for the Hilbert-Schmidt norm. For the finite dimensional Hilbert space $\mathbb{C}^n$, we use bra-ket notation and write $|0\rangle, \ldots, |n-1\rangle$ for the standard basis. We define the circle $\mathbb{S}^1 = \mathbb{R}/\mathbb{Z}$ as the interval $[0,1]$ with endpoints identified. We write $L^2(\mathbb{R})$, $L^2(\mathbb{S}^1)$, etc. for Hilbert spaces of square-integrable functions, equipped with the Lebesgue measure that assigns unit measure to unit intervals, and we denote by $\ell^2(\mathbb{Z})$ the Hilbert space of square-integrable sequences. The Fourier transform of a function $\phi \in L^2(\mathbb{R})$ is denoted by $\hat{\phi} \in L^2(\mathbb{R})$ and is given by $\hat{\phi}(\omega) = \int_{-\infty}^{\infty} f(x) e^{-ix\omega} dx$ if ϕ is absolutely integrable. Similarly, the Fourier transform of a function $\phi \in L^2(\mathbb{S}^1)$ is denoted by $\hat{\phi} \in \ell^2(\mathbb{Z})$ and can be computed as $\hat{\phi}[n] = \int_0^1 f(x) e^{-ix2\pi n} dx$. We define the Fourier transform of a sequence $f \in \ell^2(\mathbb{Z})$ to be the 2π-periodic function $\hat{f} \in L^2(\mathbb{R}/2\pi\mathbb{Z})$ given by $\hat{f}(\theta) = \sum_{n\in\mathbb{Z}} f[n] e^{-i\theta n}$. For $\mathbb{H} = L^2(\mathbb{R})$, $L^2(\mathbb{S}^1)$, $\ell^2(\mathbb{Z})$ or $\ell^2(\mathbb{Z}/m\mathbb{Z})$, and $\lambda \in \mathbb{H}$, we will denote by $m(\hat{\lambda})$ the *Fourier multiplier* with symbol $\hat{\lambda}$, defined by multiplication with $\hat{\lambda}$ in the Fourier domain (equivalently, convolution with λ in the original domain). On $\ell^2(\mathbb{Z})$, we define the *downsampling* operator $\downarrow$ by $(\downarrow f)[n] = f[2n]$;

its adjoint is the *upsampling* operator $\uparrow$ given by $(\uparrow f)[2n] = f[n]$ and $(\uparrow f)[2n+1] = 0$ for $f \in \ell^2(\mathbb{Z})$. We will also use the Sobolev spaces $H^K(\mathbb{R})$ and $H^K(\mathbb{S}^1)$, which consist of functions that have a square-integrable weak K-th derivative, denoted $f^{(K)}$. All p-norms for $p \neq 2$ will be denoted by $\|f\|_p$. We write $\mathbf{1}$ for the constant function equal to one, and $\mathbf{1}_X$ for the indicator function of a set X. If $f \in L^2(\mathbb{R})$ and has compact support, we write $D(f)$ for the size of the smallest interval containing the support of f.

2 Preliminaries

In this section, we briefly review the second quantization formalism for fermions and quasi-free fermionic many-body states (see, e.g., [44] or [45] for further details), and we describe the vacuum state of massless free fermions in $1+1$ dimensions in terms of this formalism.

2.1 The CAR algebra and quasi-free states

If $\mathbb{H}$ is a complex Hilbert space, then let $\mathcal{A}_\wedge(\mathbb{H})$ be the algebra of canonical anti-commutation relations or *CAR algebra* on $\mathbb{H}$. It is the free unital $C^\dagger$-algebra generated by elements $a(f)$ for $f \in \mathbb{H}$ such that $f \mapsto a(f)$ is anti-linear and subject to the relations

$$\{a(f), a(g)\} = 0,$$
$$\{a(f), a^\dagger(g)\} = \langle f, g\rangle$$

where $\{x, y\} = xy + yx$ denotes the anti-commutator.

An important class of states on this algebra are the *gauge-invariant quasi-free* (or *Gaussian*) states. These states have the property that they are invariant under a global phase and that all correlation functions are determined by the two-point functions. More precisely, for every operator Q on $\mathbb{H}$ such that $0 \leqslant Q \leqslant \mathbb{1}$ there exists a unique gauge-invariant quasi-free state on $\mathcal{A}_\wedge(\mathbb{H})$, denoted ω_Q, such that we have the following version of Wick's rule:

$$\omega_Q(a^\dagger(f_1)\dots a^\dagger(f_n)a(g_1)\dots a(g_m)) = \delta_{n,m}\det[\langle g_i, Qf_j\rangle]$$

Thus, the state is fully specified by its two-point functions $\omega_Q(a^\dagger(f)a(g)) = \langle g, Qf\rangle$. The operator Q is called the *symbol* of ω_Q. It is well-known that ω_Q is a pure state if and only if Q is a projection. In this case, Q can be interpreted as a projection onto a *Fermi sea* of negative energy modes. Since throughout this article we will only be interested in this case, we henceforth assume that Q is a projection.

To obtain a Hilbert space realization, we consider the fermionic Fock space

$$\mathcal{F}_\wedge(\mathbb{H}) = \bigoplus_{n=0}^{\infty} \mathbb{H}^{\wedge n}$$

with the standard representation of $\mathcal{A}_\wedge(\mathbb{H})$, defined by $a(f) \mapsto a_0(f)$ where $a_0^\dagger(f)v = f \wedge v$. Let $|\Omega\rangle$ denote the Fock vacuum vector $1 \in \mathbb{H}^{\wedge 0}$. Then $|\Omega\rangle$ is the pure state corresponding to symbol $Q = 0$. Now let Q be an arbitrary orthogonal projection and choose a complex conjugation $\overline{(\cdot)}$ (that is, an antiunitary involution) that commutes with Q. Then the map $a(f) \mapsto a_Q(f)$, where

$$a_Q(f) = a_0\big((\mathbb{1} - Q)f\big) + a_0^\dagger\big(\overline{Qf}\big), \tag{2.1}$$

defines a representation of the CAR algebra such that ω_Q corresponds to the Fock vacuum vector $|\Omega\rangle$.

2.2 Second-quantized operators

Next we recall the second quantization of operators on $\mathbb{H}$. If U is a unitary on $\mathbb{H}$ then U defines an automorphism of $\mathcal{A}_\wedge(\mathbb{H})$, known as a *Bogoliubov transformation*, through $a(f) \mapsto a(Uf)$. Provided that $[U, Q]$ is Hilbert-Schmidt, this automorphism can be implemented by a unitary operator $\Gamma_Q(U)$ on Fock space, which is unique up to an overall phase. This means that, for every $f \in \mathbb{H}$,

$$\Gamma_Q(U) a_Q(f) \Gamma_Q(U)^\dagger = a_Q(Uf).$$

Now consider a unitary one-parameter subgroup $\{e^{itA}\}$ generated by a bounded Hermitian operator A on $\mathbb{H}$. This would like to know when e^{itA} can be unitarily implemented in the form

$$e^{it d\Gamma_Q(A)} a_Q(f) e^{-it d\Gamma_Q(A)} = a_Q(e^{itA} f) \tag{2.2}$$

for $t \in \mathbb{R}$ and $f \in \mathbb{H}$. For this, decompose A into blocks with respect to $\mathbb{H}_\pm$, which we define as the range of the projections $Q_+ = \mathbb{1} - Q$ and $Q_- = Q$ (corresponding to positive and negative energy modes), respectively:

$$A = \begin{pmatrix} A_{++} & A_{+-} \\ A_{-+} & A_{--} \end{pmatrix}$$

In [45, 46] it is shown that, if A is bounded and the off-diagonal parts A_{+-}, A_{-+} are Hilbert-Schmidt, then there exists a self-adjoint generator $d\Gamma_Q(A)$ on $\mathcal{F}_\wedge(\mathbb{H})$ such that (2.2) holds. We can moreover fix the undetermined additive constant by demanding that

$$\langle \Omega, d\Gamma_Q(A) \Omega \rangle = 0,$$

which corresponds to *normal ordering* with respect to the state ω_Q.

If A is trace class then $d\Gamma_Q(A)$ is bounded and in fact can be defined as an element of $\mathcal{A}_\wedge(\mathbb{H})$. In general, $d\Gamma_Q(A)$ is unbounded, but we still have the bound [45, (2.53)]

$$\|d\Gamma_Q(A) \Pi_n\| \leqslant 4(n+2) \max\{\|A_{++}\|, \|A_{--}\|, \|A_{+-}\|_2, \|A_{-+}\|_2\}, \tag{2.3}$$

where Π_n denotes the orthogonal projection on the subspace of $\mathcal{F}_\wedge(\mathbb{H})$ spanned by states of no more than n particles. Combining [45, (2.14), (2.24), (2.25), (2.49)], one can similarly show that

$$\|\big(d\Gamma_Q(A) - d\Gamma_{Q'}(A)\big) \Pi_n\| \leqslant 4(n+2) \max_{\delta=\pm} \{\|Q_\delta A Q_\delta - Q'_\delta A Q'_\delta\|, \|Q_\delta A Q_{-\delta} - Q'_\delta A Q'_{-\delta}\|_2\} \tag{2.4}$$

for any two projections Q and Q'. This estimate will be useful in our error analysis in Section 4.2.

2.3 Massless free fermions in 1+1 dimensions

We now describe the vacuum state of the free Dirac fermion quantum field theory in $1+1$ dimensions in terms of the second quantization formalism. It will be convenient to consider the Dirac equation in the form

$$i\gamma^\mu \partial_\mu \psi = 0,$$

with the Dirac matrices $\gamma^0 = i\sigma_z = \left(\begin{smallmatrix} i & 0 \\ 0 & -i \end{smallmatrix}\right)$ and $\gamma^1 = -\sigma_x = \left(\begin{smallmatrix} 0 & -1 \\ -1 & 0 \end{smallmatrix}\right)$. The equation is easily seen to be solved by

$$\psi_1(x,t) = \chi_+(x+t) + \chi_-(x-t)$$
$$\psi_2(x,t) = i\,(\chi_+(x+t) - \chi_-(x-t))$$

for arbitrary functions χ_+ and χ_-, which we take to be in $L^2(\mathbb{R})$ in order for the solutions to be normalizable. The energy of such a solution is given by

$$E = \int_{-\infty}^{\infty} \left(-\omega|\hat{\chi}_+(\omega)|^2 + \omega|\hat{\chi}_-(\omega)|^2\right)\,d\omega.$$

Thus, the space of negative energy solutions is spanned by solutions for which χ_+ has a Fourier transform with support on the positive half-line (is analytic) and χ_- has a Fourier transform with support on the negative half-line (is anti-analytic).

We obtain a single-particle Hilbert space $\mathbb{H} = L^2(\mathbb{R}) \otimes \mathbb{C}^2$ corresponding to $\psi(x, t=0)$. The symbol of the vacuum state is given by the projection onto the 'Dirac sea' of negative energy solutions. It can be expressed as

$$Q = \frac{1}{2}\begin{pmatrix} \mathbb{1} & \mathcal{H} \\ -\mathcal{H} & \mathbb{1} \end{pmatrix} \tag{2.5}$$

in terms of the *Hilbert transform*, which is the unitary operator on $L^2(\mathbb{R})$ defined by

$$\widehat{\mathcal{H}f}(\omega) = -i\,\mathrm{sgn}(\omega)\hat{f}(\omega).$$

Indeed, it follows from $\mathcal{H}^\dagger = -\mathcal{H}$ that Q is an orthogonal projection, and $Q\psi = \psi$ if ψ is the restriction to $t = 0$ of a negative-energy solution. We further note that the symbol Q commutes with the component-wise complex conjugation on $\mathbb{H}$. We thus obtain a Fock space realization as described above in Section 2.1. The smeared Dirac field can be defined as $\Psi(f) := a_Q(f)$ for $f \in \mathbb{H}$.

We will also be interested in free Dirac fermions on the circle $\mathbb{S}^1$. In this case, we take $\mathbb{H} = L^2(\mathbb{S}^1) \otimes \mathbb{C}$. For periodic boundary conditions, the symbol Q^{per} has the same form as in (2.5), where we now let

$$\widehat{\mathcal{H}^{\mathrm{per}}f}[n] = -i\,\mathrm{sgn}(n)\hat{f}[n]$$

where there is some ambiguity in the sign function for $n = 0$ (reflecting a ground state degeneracy). For definiteness, we choose $\mathrm{sgn}(0) = 1$.

For anti-periodic boundary conditions, corresponding to the Dirac equation on the nontrivial spinor bundle over $\mathbb{S}^1$, we define a unitary operator T on $\mathbb{H}$ by $Tf(x) = e^{-i\pi x}f(x)$ for $x \in (0,1)$. Then the symbol is given by $T^\dagger Q^{\mathrm{per}} T$.

2.4 Self-dual CAR algebra and Majorana fermions

Suppose that $\mathbb{H}_+ \cong \mathbb{H}_-$, as in the preceding section. Given an anti-unitary involution C on $\mathbb{H}$ such that $CQ_\delta = Q_{-\delta}C$ for $\delta = \pm$, we can also define the following operators on $\mathcal{F}_\wedge(\mathbb{H}_+) \subset \mathcal{F}_\wedge(\mathbb{H})$,

$$c_Q(f) = a_0(Q_+ f) + a_0^\dagger(CQ_- f) \tag{2.6}$$

These satisfy the relations of the *self-dual CAR algebra*, $\mathcal{A}^{\mathrm{sd}}_{\wedge}(\mathbb{H})$ [47], which is generated by elements $c(f)$ for $f \in \mathbb{H}$ such that $f \mapsto c(f)$ is antilinear and

$$\{c(f), c^\dagger(g)\} = \langle f, g\rangle\,,$$
$$c^\dagger(f) = c(Cf).$$

for $f, g \in \mathbb{H}$. The second equation implies that a unitary U on $\mathbb{H}$ only defines an automorphism $\Gamma^c(U)$ of $\mathcal{A}^{\mathrm{sd}}_{\wedge}(\mathbb{H})$ by $c(f) \mapsto c(Uf)$ if $[U, C] = 0$ commutes with C. We can also second quantize generators as in Eq. (2.2). That is, if A is a bounded operator with Hilbert-Schmidt A_{+-}, A_{-+}, and if $A^\dagger = -CAC$, we can define its second quantization $d\Gamma^c_Q(A)$, such that

$$e^{itd\Gamma^c_Q(A)} c_Q(f) e^{-itd\Gamma^c_Q(A)} = c_Q(e^{itA} f). \tag{2.7}$$

We can apply this construction in the situation Section 2.3 to obtain a description of massless free Majorana fermions. Define the anti-unitary involution C as the following charge conjugation operator which exchanges positive and negative energy modes:

$$Cf = \begin{pmatrix} 1 & 0 \\ 0 & -1 \end{pmatrix} \bar{f} \tag{2.8}$$

Then it is clear from (2.5) that $CQ = (I - Q)C$, so the above construction applies. We denote by $\Phi(f) := c_Q(f)$ the smeared Majorana field.

3 Hilbert pair wavelets

Our circuits for free-fermion correlation functions will be obtained by second quantizing a wavelet transformation. In this section, we first review the basic theory of wavelets on the line and circle. In Section 3.1 we explain the definition of a wavelet basis, and how a choice of wavelet basis stratifies a function space into different scales. Next, in Section 3.2 we explain how these different scales are related through filters, and in Section 3.3 we explain the periodic version. An important question is how accurately a function f is approximated if all but a finite number of scales are truncated. This is discussed in Section 3.4, where we prove some results that are completely standard in the wavelet literature, but which we work out for convenience of the reader, and in order to be able to carefully keep track of all the constants involved. Using an argument from Fourier analysis in Lemma A.2 we show in Lemma 3.1 an approximation result for a 'UV cut-off' for a sufficiently smooth f, where we discard all detail at fine scales, or alternatively in Lemma 3.2, if we sample f. Next we show in Lemma 3.3 that for compactly supported functions we can also discard large scale wavelet components up to a small error, which should be thought of as an 'IR cut-off'. Finally, in Section 3.5 we introduce a way to implement the Hilbert transform using wavelets. Since we want to use compactly supported wavelets, this can only be done approximately, and in Lemma 3.5, Lemma 3.6 and Lemma 3.7 we the bound approximation errors this gives rise to.

For a more extensive introduction to wavelets we refer the reader to, e.g., Chapter 7 in [48]. We then define the central notion of an *approximate Hilbert pair* of wavelet filters (Definition 3.4) and derive some estimates that will later be used to derive our first-quantized approximation results.

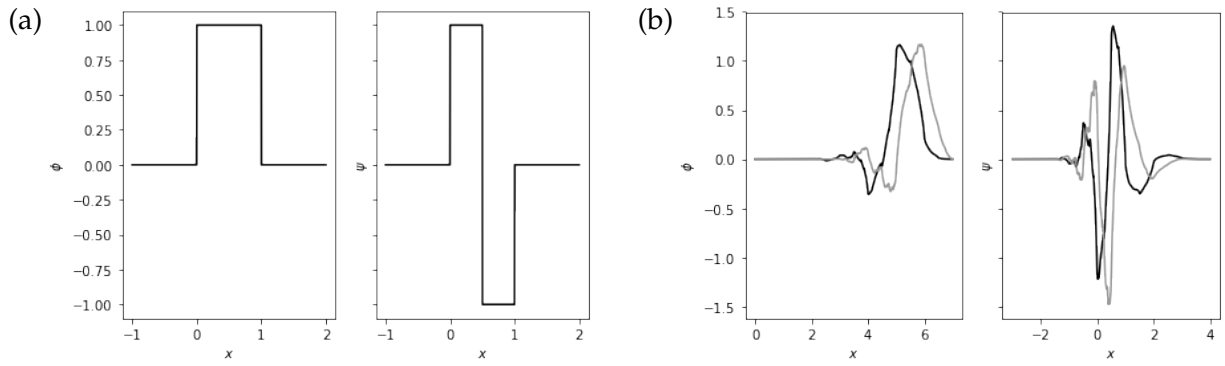

Figure 4: (a) Scaling and wavelet function for the Haar wavelet ($\phi = \mathbf{1}_{[0,1)}$, $\psi = \mathbf{1}_{[0,\frac{1}{2})} - \mathbf{1}_{[\frac{1}{2},1)}$). (b) Scaling and wavelet functions for the approximate Hilbert pair with parameters $K = L = 2$ due to Selesnick (ϕ^h, ψ^h in black; ϕ^g, ψ^g in gray). See Section 3.5 and Table 2 for further detail.

3.1 Wavelet bases

A wavelet basis is an orthonormal basis for $L^2(\mathbb{R})$ consisting of scaled and translated versions of a single localized function $\psi \in L^2(\mathbb{R})$, called the *wavelet function*. If we define

$$W_j = \sup\{\psi_{j,k} : k \in \mathbb{Z}\}, \quad \text{where} \quad \psi_{j,k}(x) = 2^{\frac{j}{2}}\psi(2^j x - k),$$

then $L^2(\mathbb{R}) = \bigoplus_j W_j$. We can therefore interpret of W_j as the *space of functions at scale* j, also called the detail space at scale j, where large j corresponds to fine scales and small j to coarse scales.

In signal processing, wavelet bases are often constructed from an auxiliary function $\phi \in L^2(\mathbb{R})$, known as the *scaling function*. To be precise, we demand that the V_j form a complete filtration of $L^2(\mathbb{R})$, i.e.,

$$\{0\} \subseteq \ldots \subseteq V_j \subseteq V_{j+1} \subseteq \ldots \subseteq L^2(\mathbb{R}), \quad \overline{\bigcup_j V_j} = L^2(\mathbb{R}),$$

and that the wavelets at scale j span exactly the orthogonal complement of V_j in V_{j+1}:

$$V_{j+1} = W_j \oplus V_j \tag{3.1}$$

for all $j \in \mathbb{Z}$. A sequence of subspaces $\{V_j\}_{j\in\mathbb{Z}}$ as above is said to form a *multiresolution analysis*, since Eq. (3.1) allows to recursively decompose a signal in some V_j scale by scale. The orthogonality between scaling and wavelet function is well-illustrated by the *Haar wavelet* (see Fig. 4, (a)), which was used in Qi's exact holographic mapping [24]. We will use pairs of wavelets that are tailored to target the vacuum of the Dirac theory (see Section 3.5 below).

Wavelet bases as above can be obtained by deriving them from filters. A sequence $g_s \in \ell^2(\mathbb{Z})$ is called a *scaling filter* (or *low-pass filter*) if its Fourier transform satisfies, for all $\theta \in \mathbb{R}/2\pi\mathbb{Z}$,

$$|\hat{g}_s(\theta)|^2 + |\hat{g}_s(\theta+\pi)|^2 = 2 \quad \text{and} \quad \hat{g}_s(0) = \sqrt{2}. \tag{3.2}$$

Under mild technical conditions on g_s (see, e.g., [48, Thm 7.2]), which we always assume to be satisfied, we can define scaling and wavelet functions $\phi, \psi \in L^2(\mathbb{R})$ such that

$$\psi(x) = \sqrt{2}\sum_{n\in\mathbb{Z}} g_w[n]\phi(2x-n),$$

$$\phi(x) = \sqrt{2} \sum_{n \in \mathbb{Z}} g_s[n] \phi(2x - n).$$

The sequence $g_w \in \ell^2(\mathbb{Z})$ is known as the *wavelet filter* (or *high-pass filter*) and it can be computed via

$$\hat{g}_w(\theta) = e^{-i\theta} \overline{\hat{g}_s(\theta + \pi)}, \quad \text{i.e.} \quad g_w[n] = (-1)^{1-n} \bar{g}_s[1-n]. \tag{3.3}$$

Thus, the expansion coefficients of the wavelet and scaling function at scale $j = 0$ in terms of scaling functions at scale $j = 1$ are precisely given by the wavelet and scaling filters, respectively (cf. Eq. (3.1)). This generalizes immediately to arbitrary scales: For all $j, k \in \mathbb{Z}$,

$$\psi_{j,k} = \sum_{n \in \mathbb{Z}} g_w[n] \phi_{j+1,2k+n}, \tag{3.4}$$

$$\phi_{j,k} = \sum_{n \in \mathbb{Z}} g_s[n] \phi_{j+1,2k+n}. \tag{3.5}$$

In Fourier space, these relations read

$$\hat{\psi}(\omega) = \frac{1}{\sqrt{2}} \hat{g}_w\Big(\frac{\omega}{2}\Big) \hat{\phi}\Big(\frac{\omega}{2}\Big), \tag{3.6}$$

$$\hat{\phi}(\omega) = \frac{1}{\sqrt{2}} \hat{g}_s\Big(\frac{\omega}{2}\Big) \hat{\phi}\Big(\frac{\omega}{2}\Big) \tag{3.7}$$

for all $\omega \in \mathbb{R}$. The Fourier transform of the scaling function can be expressed as an infinite product of evaluations of the scaling filter:

$$\hat{\phi}(\omega) = \prod_{k=1}^{\infty} \frac{1}{\sqrt{2}} \hat{g}_s(2^{-k}\omega) \tag{3.8}$$

In particular, it is bounded by one, i.e., $\|\hat{\phi}\|_\infty = 1$. It is also useful to note that the wavelet function averages to zero, i.e., $\int_{-\infty}^{\infty} \psi(x) dx = 0$.

Throughout this article, we will always work with filters of *finite length* (the length of a sequence $f \in \ell^2(\mathbb{Z})$ is defined as the minimal number M such that f is supported on M consecutive sites). Specifically, we will assume that the support of the scaling filter is $\{0, \dots, M-1\}$. In the signal processing literature, such filters are called finite impulse response (FIR) filters with M taps. It is clear from Eq. (3.3) that in this case the wavelet filter is supported in $\{2-M, \dots, 1\}$, hence has finite length M as well. If the filters have finite length then the wavelet and scaling functions are compactly supported on intervals of width M [48, Prop 7.2].

3.2 Wavelet decompositions

Suppose that we would like to express a given function $f \in L^2(\mathbb{R})$ in a wavelet basis. As a first step, we replace f by $P_j f \in V_j$, where $P_j \colon L^2(\mathbb{R}) \to V_j$ denotes the orthogonal projection onto the space of functions below scale j. This is corresponds to removing high frequency components (in signal processing) or to a UV cut-off (in physics). We explain in Lemma 3.1 below how to bound the error $\|f - P_j f\|$ in terms of a Sobolev norm. To express $P_j f$ in terms of the orthonormal basis $\{\phi_{j,k}\}_{k \in \mathbb{Z}}$ of V_j, define the partial isometries

$$\alpha_j \colon L^2(\mathbb{R}) \to \ell^2(\mathbb{Z}), \qquad (\alpha_j f)[k] = \langle \phi_{j,k}, f \rangle, \tag{3.9}$$

where we note that $P_j = \alpha_j^\dagger \alpha_j$. We show below that, if f is sufficiently smooth, the coefficients $\alpha_j f$ can be well-approximated by sampling f on a uniform grid with spacing 2^{-j} (Lemma 3.2).

Next, we iteratively obtain the wavelet coefficients of $P_j f$ at all scales $n < j$. For this purpose, let

$$\beta_j \colon L^2(\mathbb{R}) \to \ell^2(\mathbb{Z}), \quad (\beta_j f)[k] = \langle \psi_{j,k}, f \rangle ,$$

and define the unitary operator

$$W \colon \ell^2(\mathbb{Z}) \to \ell^2(\mathbb{Z}) \otimes \mathbb{C}^2, \qquad Wf = (\downarrow m(\overline{\hat{g}_w})f) \oplus (\downarrow m(\overline{\hat{g}_s})f), \tag{3.10}$$

where we recall that the downsampling operator is given by $(\downarrow f)[n] = f[2n]$. Then, Eqs. (3.4) and (3.5) imply that

$$W\alpha_{j+1} f = \beta_j f \oplus \alpha_j f$$

for all $f \in L^2(\mathbb{R})$ and $j \in \mathbb{Z}$. That is, applying W to the scaling coefficients at some scale j yields in the first component the wavelet coefficients and in the second component the scaling coefficients at one scale coarser. Note that, due to the scale invariance of the wavelet basis, the operator W does *not* depend explicitly on j. We can iterate this procedure to obtain a map

$$W^{(\mathcal{L})} \colon \ell^2(\mathbb{Z}) \to \ell^2(\mathbb{Z}) \otimes \mathbb{C}^{\mathcal{L}+1}, \qquad W^{(\mathcal{L})} = (\mathbb{1}_{\ell^2(\mathbb{Z})\otimes\mathbb{C}^{\mathcal{L}-1}} \oplus W) \cdots (\mathbb{1}_{\ell^2(\mathbb{Z})} \oplus W)W, \tag{3.11}$$

which decomposes through successive filtering the scaling coefficients at scale $j+1$ into the wavelet coefficients at scales j to $j - \mathcal{L} + 1$ and the scaling coefficients at scale $j - \mathcal{L} + 1$. That is:

$$W^{(\mathcal{L})}\alpha_{j+1} = \beta_j \oplus W^{(\mathcal{L}-1)}\alpha_j = \cdots = \beta_j \oplus \beta_{j-1} \oplus \ldots \oplus \beta_{j-\mathcal{L}+1} \oplus \alpha_{j-\mathcal{L}+1},$$

or

$$W^{(\mathcal{L})}\alpha_{j+1} f = \sum_{l=0}^{\mathcal{L}-1} \beta_{j-l+1} f \otimes |l\rangle + \alpha_{j-\mathcal{L}+1} f \otimes |\mathcal{L}\rangle$$

for all $f \in L^2(\mathbb{R})$. The unitaries W and $W^{(\mathcal{L})}$ are known as ($\mathcal{L}$ layers of) the *discrete wavelet transform*. Note that $W^{(\mathcal{L})}$ can be readily implemented by a scale-invariant linear circuit consisting of convolutions and downsampling circuit elements (see Section 5.3 and Fig. 5 for a visualization).

3.3 Periodic wavelets

Given a wavelet ψ on $\mathbb{R}$ with scaling function ϕ and filters g_s and g_w, one can construct a corresponding family of *periodic* wavelet and scaling functions on the circle $\mathbb{S}^1$. Following [48, Section 7.5], we define for $j \geqslant 0$ and $k = 1, \ldots, 2^j$ the functions

$$\psi^{\mathrm{per}}_{j,k}(x) = \sum_{m\in\mathbb{Z}} \psi_{j,k}(x + m),$$
$$\phi^{\mathrm{per}}_{j,k}(x) = \sum_{m\in\mathbb{Z}} \phi_{j,k}(x + m)$$

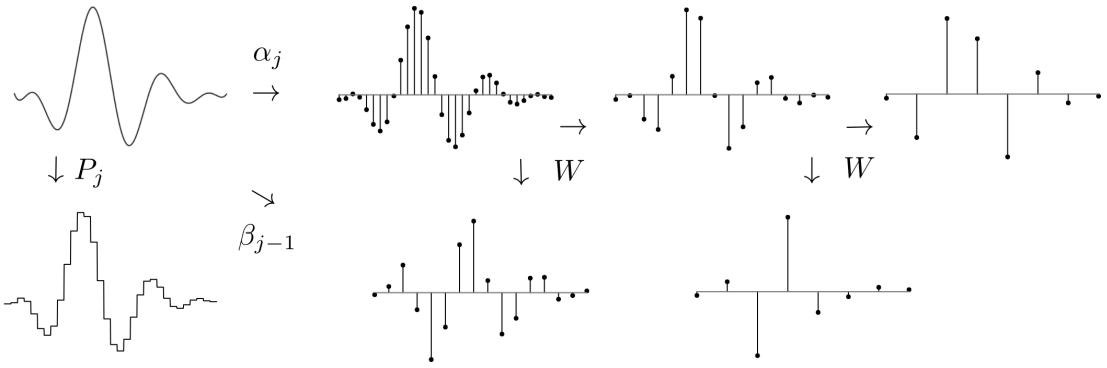

Figure 5: Illustration of the various maps defined in Section 3.2 in the case of the Haar wavelet.

in $L^2(\mathbb{S}^1)$. If we set $V_j^{\mathrm{per}} = \mathrm{span}\{\phi_{j,k}^{\mathrm{per}} : k = 1, \dots, 2^j\}$ and $W_j^{\mathrm{per}} = \mathrm{span}\{\psi_{j,k}^{\mathrm{per}} : k = 1, \dots, 2^j\}$ then we have

$$\mathbb{C}\mathbf{1} = V_0 \subseteq V_1 \subseteq \cdots \subseteq L^2(\mathbb{S}^1), \quad \overline{\bigcup_{j \geqslant 0} V_j} = L^2(\mathbb{S}^1), \quad \text{and} \quad V_{j+1} = W_j \oplus V_j.$$

The space V_0 is one-dimensional and consists of the constant functions. Thus, $\{\psi_{j,k}^{\mathrm{per}}\}_{j \geqslant 0, k=1,\dots,2^j}$ together with $\phi_{0,1}^{\mathrm{per}} = \mathbf{1}$ form an orthonormal basis of $L^2(\mathbb{S}^1)$. Similarly to before, we denote by $\alpha_j^{\mathrm{per}}, \beta_j^{\mathrm{per}} \colon L^2(\mathbb{S}^1) \to \mathbb{C}^{2^j}$ denote the partial isometries that send a function to its expansion coefficients with respect to the periodized scaling and wavelet basis functions (for fixed j), and we denote by $P_j^{\mathrm{per}} = (\alpha_j^{\mathrm{per}})^\dagger \alpha_j^{\mathrm{per}}$ to be the orthogonal projection onto $V_j \subseteq L^2(\mathbb{S}^1)$.

Since the radius of the circle sets a coarsest length scale, the corresponding filters are now scale-dependent and given by

$$g_{s,j}^{\mathrm{per}}[n] = \sum_{m \in \mathbb{Z}} g_s[n + 2^j m]$$
$$g_{w,j}^{\mathrm{per}}[n] = \sum_{m \in \mathbb{Z}} g_w[n + 2^j m]$$

for $j \geqslant 0$ and $n = 1, \dots, 2^j$. As before, they give rise to unitary maps

$$W^{(\mathcal{L}),\mathrm{per}} \colon \mathbb{C}^{2^{\mathcal{L}}} \to \bigoplus_{j=0}^{\mathcal{L}-1} \mathbb{C}^{2^j} \oplus \mathbb{C}, \quad W^{(\mathcal{L}),\mathrm{per}} \alpha_{\mathcal{L}}^{\mathrm{per}} = \beta_{\mathcal{L}-1}^{\mathrm{per}} \oplus \ldots \oplus \beta_0^{\mathrm{per}} \oplus \alpha_0^{\mathrm{per}} \tag{3.12}$$

that expand a signal at a certain scale into (all) its wavelet coefficients and the remaining scaling coefficient (which is the average of f).

We note that $g_{s,j}^{\mathrm{per}} = g_s$ and $g_{w,j}^{\mathrm{per}} = g_w$ for sufficiently large j (namely when 2^j is at least as large as the cardinality of the filters' supports). This is intuitive since at sufficiently fine scales the periodicity of the circle is no longer visible. See Section 5.3 for more detail.

3.4 Wavelet approximations

We need to know how well we can approximate functions if we are only allowed to use a finite number of scales. In this section we will state three results (the last of which is adapted from [49]) that

give quantitative bounds assuming that the wavelets are compactly supported and bounded. These conditions can easily be relaxed, but we will not need this. The proofs are given in Appendix A.

Our first result bounds the error incurred by leaving out detail, corresponding to a UV cut-off. Recall that the Sobolev spaces $H^K(\mathbb{R})$ and $H^K(\mathbb{S}^1)$ consist of functions f with square-integrable weak K-th derivative, denoted $f^{(K)}$.

Lemma 3.1 (UV cut-off)**.** *Assume that the Fourier transform of the scaling filter $\hat{g}_s(\theta)$ has a zero of order K at $\theta = \pi$. Then there exists a constant C_{UV} such that for every $f \in H^K(\mathbb{R})$ and $j \in \mathbb{Z}$, we have that*

$$\|P_j f - f\| \leqslant 2^{-Kj} C_{UV} \|f^{(K)}\|.$$

Similarly, for every $f \in H^1(\mathbb{S}^1)$ and $j \geqslant 0$, we have that

$$\|P_j^{\mathrm{per}} f - f\| \leqslant 2^{-Kj} C_{UV} \|f^{(K)}\|.$$

If the scaling filter is supported in $\{0, \ldots, M-1\}$, then these estimates hold with $K = 1$ and $C_{UV} \leqslant 2M^2$.

In fact, under mild technical conditions the 'UV cut-off' from Lemma 3.1 can be well-approximated by sampling the function on a dyadic grid, as shown in the following lemma.

Lemma 3.2 (Sampling error)**.** *There exists a constant C_ϕ such that the following holds: For every $f \in H^1(\mathbb{R})$ and f_j the sequence defined by $(f_j)_k := 2^{-j/2} f(2^{-j}k)$ for $k \in \mathbb{Z}$ (we identify f with its unique representative as a continuous function), we have*

$$\|\alpha_j f - f_j\| \leqslant 2^{-j} C_\phi \|f'\|.$$

Likewise, for every $f \in H^1(\mathbb{S}^1)$ and $f_j \in \mathbb{C}^{2^j}$ the vector with components $(f_j)_k := 2^{-j/2} f(2^{-j}k)$,

$$\|\alpha_j^{\mathrm{per}} f - f_j\| \leqslant 2^{-j} C_\phi \|f'\|.$$

If the scaling filter is supported in $\{0, \ldots, M-1\}$, then these estimates hold with $C_\phi \leqslant 2M^2$.

The final lemma of this section bounds the error incurred by leaving out coarse scale components from compactly supported functions, corresponding to an IR cut-off.

Lemma 3.3 (IR cut-off)**.** *Assume that the scaling function ϕ satisfies*

$$\sqrt{\sum_{k \in \mathbb{Z}} |\phi(y-k)|^2} \leqslant C_{IR}$$

for all $y \in \mathbb{R}$. Then for every $f \in L^2(\mathbb{R})$ with compact support,

$$\|P_j f\| \leqslant 2^{j/2} \sqrt{D(f)} C_{IR} \|f\|.$$

In particular, if ϕ is bounded and supported in an interval of width M, this is true with $C_{IR} \leqslant \sqrt{M}\|\phi\|_\infty$.

We recall from Section 3.1 that both the scaling and the wavelet function are supported on intervals of the same width, which explains why we use the symbol M in both cases. For the periodized wavelet transform, it is possible to prove a similar result when restricting to functions $f \in L^2(\mathbb{S}^1)$ with average zero (since the identity function is orthogonal to all wavelet basis functions).

3.5 Approximate Hilbert pair wavelets

Our construction of a quantum circuit that approximates fermionic correlation functions is based on approximating the Hilbert transform, which we saw appearing in the symbol in Section 2.3, by using wavelets. Thus, we are looking for a pair of wavelet and scaling filters g_w, g_s and h_w, h_s such that the associated wavelet functions ψ^g and ψ^h satisfy

$$\psi^h = \mathcal{H}\psi^g,$$

which we recall means that $\hat{\psi}^h(\omega) = -i\,\mathrm{sgn}(\omega)\hat{\psi}^g(\omega)$ for all $\omega \in \mathbb{R}$. Such a pair of wavelets is called a *Hilbert pair*. Two equivalent conditions on the scaling and wavelet filters, respectively, to generate a Hilbert pair are [50]

$$\begin{aligned} \hat{h}_s(\theta) &= \mu_s(\theta)\hat{g}_s(\theta), \\ \hat{h}_w(\theta) &= \mu_w(\theta)\hat{g}_w(\theta), \end{aligned} \tag{3.13}$$

where μ_s and μ_w are periodic functions in $L^\infty(\mathbb{R}/2\pi\mathbb{Z})$ defined by

$$\begin{aligned} \mu_s(\theta) &= e^{-i\frac{\theta}{2}}, \\ \mu_w(\theta) &= -i\,\mathrm{sgn}(\theta)e^{i\frac{\theta}{2}} \end{aligned} \tag{3.14}$$

for $|\theta| < \pi$. In this situation, Eqs. (3.6) and (3.7) implies that the scaling functions ϕ_g and ϕ_h will be related by

$$\hat{\phi}^h(\omega) = \lambda_s(\omega)\hat{\phi}^g(\omega), \tag{3.15}$$

where $\lambda_s \in L^\infty(\mathbb{R})$ is defined by

$$\lambda_s(\omega) = -i\,\mathrm{sgn}(\omega)\mu_w(-\omega). \tag{3.16}$$

We refer to [29, 50] for further detail. Since the Hilbert transform does not preserve compact support, we can not hope for exact Hilbert pair wavelets using compactly supported wavelets. However, an approximate version can be realized. The following definition describes the notion of approximation that is appropriate in our context.

Definition 3.4. An *ε-approximate Hilbert pair* consists of a pair of wavelet and scaling filters, g_w, g_s, h_w, h_s, with corresponding wavelet functions ψ^g, ψ^h and scaling functions ϕ^g, ϕ^h, such that

$$\|\hat{h}_s - \mu_s\hat{g}_s\|_\infty \leqslant \varepsilon. \tag{3.17}$$

That is, the error in the phase relation (3.13) for the scaling filters is bounded by ε. This condition can readily be checked numerically.

One of the first systematic constructions of approximate Hilbert pairs is due to Selesnick [29, 50]. His construction depends on two parameters, K and L, where K is the number of vanishing moments of the wavelets (relevant for the approximation power of the wavelet decomposition and for the smoothness of the wavelets) and where L is essentially the number of terms in a Taylor expansion of the relation in Eq. (3.13) at $\theta = 0$. By construction, the filters are real and have finite length $M = 2(K + L)$, so the wavelet and scaling functions are compactly supported on intervals of

K	L	M	ε	C_{UV}	C_{IR}	C_χ	C'_χ	C_ϕ
1	1	4	0.264099	0.619741	2.542073	1.166423	1.142220	1.254999
2	2	8	0.068221	0.622182	1.217454	1.155488	0.295133	2.296890
3	3	12	0.018338	0.624782	1.190944	1.154757	0.079283	2.116091
4	4	16	0.005020	0.626782	1.150151	1.154705	0.021691	1.251461
5	5	20	0.001389	0.628374	1.130260	1.154701	0.005999	2.120782
6	6	24	0.000387	0.629686	1.120354	1.154701	0.001671	2.106891
7	7	28	0.000108	0.630795	1.114293	1.154701	0.000468	1.234832
8	8	32	0.000030	0.631752	1.108135	1.154701	0.000132	2.434899
9	9	36	0.000009	0.632674	1.106718	1.154701	0.000037	1.923738
10	10	40	0.000003	0.638023	1.440101	1.154701	0.000011	5.752427

Table 2: Numerical values of various constants for Selesnick's approximate Hilbert pairs with parameters $K = L$. It appears that ε decays exponentially with increasing $K = L$, while the other constants from Lemma 3.1, Lemma 3.2, Lemma 3.3 and Lemma 3.7 are well-behaved.

width M. Numerically, one can see that the parameter ε in Eq. (3.17) decays exponentially with $\min\{K, L\}$ [13], while the other relevant parameters from Lemma 3.1, Lemma 3.2 and Lemma 3.3 remain bounded or grow much more slowly than the worst-case bounds that we provided, as can be seen in Table 2.

If we periodize an (approximate) Hilbert pair as described in Section 3.3, we get periodic wavelets that are (approximately) related by the Hilbert transform on the circle. The following lemma is an improved version of [13, (A7)]. It controls the error incurred by using approximate instead of exact Hilbert pairs both on the line and on the circle.

Lemma 3.5. *Consider an ε-approximate Hilbert pair. Let $W_g^{(\mathcal{L})}$ and $W_h^{(\mathcal{L})}$ denote the corresponding wavelet transforms for $\mathcal{L}$ layers, defined as in Eqs.* (3.10) *and* (3.11) *using the filters g and h, respectively. Then,*

$$\|P_w\big(W_g^{(\mathcal{L})} - W_h^{(\mathcal{L})} m(\mu_w)\big)\| \leqslant \varepsilon\mathcal{L}, \tag{3.18}$$

$$\|P_s\big(W_g^{(\mathcal{L})} - W_h^{(\mathcal{L})} m(\mu_w)\big) f\| \leqslant \varepsilon\mathcal{L}\|f\| + 2\|P_s W_g^{(\mathcal{L})} f\| \qquad (\forall f \in \ell^2(\mathbb{Z})), \tag{3.19}$$

where $P_w = \mathbb{1}_{\ell^2(\mathbb{Z})} \otimes \sum_{k=0}^{\mathcal{L}-1} |k\rangle\langle k|$ denotes the projection onto the wavelet coefficients and $P_s = \mathbb{1} - P_w$ the projection onto the scaling coefficients.

Proof. As in Eq. (3.10), denote by $W_g, W_h \colon \ell^2(\mathbb{Z}) \to \ell^2(\mathbb{Z}) \otimes \mathbb{C}^2$ the unitaries corresponding to a single layer of the wavelet transform:

$$W_g = (\downarrow m(\overline{\widehat{g}_w})) \oplus (\downarrow m(\overline{\widehat{g}_s})) \quad \text{and} \quad W_h = (\downarrow m(\overline{\widehat{h}_w})) \oplus (\downarrow m(\overline{\widehat{h}_s}))$$

One may easily verify the relation

$$m(\mu_w) \downarrow m(\mu_s) = \downarrow m(\mu_w).$$

This allows us to rewrite

$$\begin{aligned} W_h m(\mu_w) &= (\downarrow m(\overline{\widehat{h}_w})) \oplus (\downarrow m(\overline{\widehat{h}_s}))m(\mu_w) \\ &= (\downarrow m(\mu_w\overline{\widehat{h}_w})) \oplus (\downarrow m(\mu_w)m(\overline{\widehat{h}_s})) \\ &= (\downarrow m(\mu_w\overline{\widehat{h}_w})) \oplus (m(\mu_w) \downarrow m(\mu_s\overline{\widehat{h}_s})) \\ &= (\mathbb{1}_{\ell^2(\mathbb{Z})} \oplus m(\mu_w))\tilde{W}_h, \end{aligned} \tag{3.20}$$

where we introduced

$$\tilde{W}_h := (\downarrow m(\mu_w\overline{\widehat{h}_w})) \oplus (\downarrow m(\mu_s\overline{\widehat{h}_s})).$$

Now consider $\mathcal{L}$ layers of the transform. For $l = 1, \dots, \mathcal{L}$, define $W_g^l := \mathbb{1}_{\ell^2(\mathbb{Z})\otimes\mathbb{C}^{l-1}} \oplus W_g$ and similarly W_h^l and $\tilde{W}_h^l$, so that $W_g^{(\mathcal{L})} = W_g^{\mathcal{L}} \cdots W_g^1$ etc. By using Eq. (3.20), we find that

$$W_h^{(\mathcal{L})} m(\mu_w) = W_h^{\mathcal{L}} \cdots W_h^1 m(\mu_w) = \left(\mathbb{1}_{\ell^2(\mathbb{Z})\otimes\mathbb{C}^{\mathcal{L}}} \oplus m(\mu_w)\right) \tilde{W}_h^{\mathcal{L}} \cdots \tilde{W}_h^1$$

Our assumption (3.17) on the scaling filter error in an approximate Hilbert pair implies that, for all l,

$$\|W_g^l - \tilde{W}_h^l\| = \|W_g - \tilde{W}_h\| \leqslant \max\{\|\overline{\widehat{g}_s} - \mu_s\overline{\widehat{h}_s}\|_\infty, \|\overline{\widehat{g}_w} - \mu_w\overline{\widehat{h}_w}\|_\infty\} \leqslant \varepsilon. \tag{3.21}$$

Next we write a telescoping sum

$$\begin{aligned} &W_g^{(\mathcal{L})} - W_h^{(\mathcal{L})} m(\mu_w) = W_g^{\mathcal{L}} \cdots W_g^1 - \left(\mathbb{1}_{\ell^2(\mathbb{Z})\otimes\mathbb{C}^{\mathcal{L}}} \oplus m(\mu_w)\right) \tilde{W}_h^{\mathcal{L}} \cdots \tilde{W}_h^1 \\ &= \left(\mathbb{1}_{\ell^2(\mathbb{Z})\otimes\mathbb{C}^{\mathcal{L}}} \oplus m(\mu_w)\right) \left(W_g^{\mathcal{L}} \cdots W_g^1 - \tilde{W}_h^{\mathcal{L}} \cdots \tilde{W}_h^1\right) + \left(0_{\ell^2(\mathbb{Z})\otimes\mathbb{C}^{\mathcal{L}}} \oplus (\mathbb{1} - m(\mu_w))\right) W_g^{\mathcal{L}} \cdots W_g^1 \\ &= \left(\mathbb{1}_{\ell^2(\mathbb{Z})\otimes\mathbb{C}^{\mathcal{L}}} \oplus m(\mu_w)\right) \sum_{l=1}^{\mathcal{L}} W_g^{\mathcal{L}} \cdots W_g^{l+1} \left(W_g^l - \tilde{W}_h^l\right) \tilde{W}_h^{l-1} \cdots \tilde{W}_h^1 + \left(0 \oplus (\mathbb{1} - m(\mu_w))\right) W_g^{\mathcal{L}} \cdots W_g^1 \end{aligned}$$

Using Eq. (3.21) and the fact that $\|W_g^l\| = \|\tilde{W}_h^l\| = 1$ for all l, we can therefore bound

$$\|P_w\left(W_g^{(\mathcal{L})} - W_h^{(\mathcal{L})} m(\mu_w)\right)\| \leqslant \sum_{l=1}^{\mathcal{L}} \|W_g^l - \tilde{W}_h^l\| \leqslant \varepsilon\mathcal{L}$$

and, since furthermore $\|m(\mu_w)\| = 1$,

$$\|P_s\left(W_g^{(\mathcal{L})} - W_h^{(\mathcal{L})} m(\mu_w)\right) f\| \leqslant \sum_{l=1}^{\mathcal{L}} \|W_g^l - \tilde{W}_h^l\| \|f\| + 2\|P_s W_g^{\mathcal{L}} \cdots W_g^1 f\| \leqslant \varepsilon\mathcal{L}\|f\| + 2\|P_s W_g^{(\mathcal{L})} f\|.$$

Thus we have established the desired bounds. □

A completely similar argument establishes a version for the periodized wavelets:

Lemma 3.6. *Consider an ε-approximate Hilbert pair. Let $W_g^{(\mathcal{L}),\mathrm{per}}$ and $W_h^{(\mathcal{L}),\mathrm{per}}$ denote the periodized wavelet transforms for $\mathcal{L}$ layers, defined as in Eq.* (3.12) *using the periodizations of the filters g and h, respectively. Then,*

$$\|P_w^{\mathrm{per}}\left(W_g^{(\mathcal{L}),\mathrm{per}} - W_h^{(\mathcal{L})} m(\mu_{w,\mathcal{L}}^{\mathrm{per}})\right)\| \leqslant \varepsilon\mathcal{L}, \tag{3.22}$$

$$\|P_s^{\mathrm{per}}\big(W_g^{(\mathcal{L}),\mathrm{per}} - W_h^{(\mathcal{L})} m(\mu_{w,\mathcal{L}}^{\mathrm{per}})\big) f\| \leqslant \varepsilon \mathcal{L} \|f\| + 2\|P_s^{\mathrm{per}} W_g^{(\mathcal{L}),\mathrm{per}} f\| \qquad (\forall f \in \mathbb{C}^{2^{\mathcal{L}}}), \tag{3.23}$$

and where P_w^{per} *denotes the projection onto the* $2^{\mathcal{L}} - 1$ *many wavelet coefficients and* $P_s^{\mathrm{per}} = \mathbb{1} - P_w^{\mathrm{per}}$ *the projection onto the remaining scaling coefficient.*

Next, we will show that expanding a function f in the scaling basis for an approximate Hilbert pair results in approximately the same coefficients as if one were to expand the function in the scaling basis for an exact Hilbert pair (cf. Eq. (3.15)).

Lemma 3.7. *Consider an* ε*-approximate Hilbert pair. Then there exists a constant* $C_\chi > 0$*, depending only on the scaling filters, such that the following holds: For every* $f \in H^1(\mathbb{R})$*,*

$$\|\alpha_j^h f - \alpha_j^g m(\lambda_{s,j})^\dagger f\| \leqslant 2^{-j} C_\chi \|f'\|.$$

where $\lambda_{s,j}(\omega) := \lambda_s(2^{-j}\omega)$*. Similarly, for* $f \in H^1(\mathbb{S}^1)$ *we have that*

$$\|\alpha_j^{h,\mathrm{per}} f - \alpha_j^{g,\mathrm{per}} m(\lambda_{s,j}^{\mathrm{per}})^\dagger f\| \leqslant 2^{-j} C_\chi \|f'\|.$$

where . If the scaling filters are supported in $\{0, \dots, M-1\}$ *then these bounds hold with* $C_\chi \leqslant 2M^2$*.*

Proof. By Eqs. (3.2) and (3.14), $\hat{h}_s - \mu_s \hat{g}_s$ vanishes at $\theta = 0$, so there exists a constant $C > 0$ such that

$$\frac{1}{\sqrt{2}} |\hat{h}_s(\theta) - \mu_s(\theta)\hat{g}_s(\theta)| \leqslant C|\theta| \tag{3.24}$$

for all $\theta \in [-\pi, \pi]$. As a consequence, we can derive the following bound on the Fourier transform of $\chi := \phi^h - m(\lambda_s)\phi^g$: For all $\omega \in [-\pi, \pi]$,

$$\begin{aligned} |\hat{\chi}(\omega)| &= |\hat{\phi}^h(\omega) - \lambda_s(\omega)\hat{\phi}^g(\omega)| = |\prod_{k=1}^{\infty} \frac{1}{\sqrt{2}} \hat{h}_s(2^{-k}\omega) - \prod_{k=1}^{\infty} \frac{1}{\sqrt{2}} \mu_s(2^{-k}\omega)\hat{g}_s(2^{-k}\omega)| \\ &\leqslant \sum_{k=1}^{\infty} \frac{1}{\sqrt{2}} |\hat{h}_s(2^{-k}\omega) - \mu_s(2^{-k}\omega)\hat{g}_s(2^{-k}\omega)| \leqslant \sum_{k=1}^{\infty} C|2^{-k}\omega| \leqslant C|\omega| \end{aligned} \tag{3.25}$$

using a telescoping series and the fact that $\|\hat{h}_s\|_\infty = \|\mu_s \hat{g}_s\|_\infty = \sqrt{2}$. Moreover, $\|\hat{\chi}\|_\infty \leqslant 2$. Thus, Lemma A.2 shows that, for all $f \in H^1(\mathbb{R})$,

$$\|\alpha_j^h f - \alpha_j^g m(\lambda_{s,j})^\dagger f\|^2 = \sum_{k \in \mathbb{Z}} |\langle \phi_{j,k}^h, f\rangle - \langle \phi_{j,k}^g, m(\lambda_{s,j})^\dagger f\rangle|^2 \quad = \sum_{k \in \mathbb{Z}} |\langle \chi_{j,k}, f\rangle|^2 \leqslant 2^{-2j} C_\chi^2 \|f'\|^2,$$

where $C_\chi^2 = C^2 + 4/3$. The case when $f \in H^1(\mathbb{S}^1)$ works analogously.

Finally, assume that the scaling filters are supported in $\{0, \dots, M-1\}$. In this case, we know from Lemma A.1 that, for all $\theta \in [-\pi, \pi]$,

$$\frac{1}{\sqrt{2}} |\hat{g}_s(\theta) - 1| \leqslant \frac{M^2}{2} |\theta| \quad \text{and} \quad \frac{1}{\sqrt{2}} |\hat{h}_s(\theta) - 1| \leqslant \frac{M^2}{2} |\theta|$$

and hence

$$\frac{1}{\sqrt{2}} |\hat{h}_s(\theta) - \mu_s(\theta)\hat{g}_s(\theta)| \leqslant \frac{1}{\sqrt{2}} |\hat{h}_s(\theta) - 1| + \frac{1}{\sqrt{2}} |\hat{g}_s(\theta) - 1| + \frac{1}{\sqrt{2}} |1 - \mu_s(-\theta)| \leqslant \left(M^2 + \frac{1}{2}\right) |\theta|$$

for $\theta \in [-\pi, \pi]$. Thus Eqs. (3.24) and (3.25) hold with $C = M^2 + 1/2$, hence we have $C_\chi \leqslant 2M^2$. □

The bounds in Lemma 3.7 hold for any pair of wavelets, not only for approximate Hilbert pairs. For the latter, not only is the constant C small in practice, but one can also use the relation between the filters Eq. (3.17) and a slightly adapted version of Lemma A.2 to show that in fact Lemma 3.7 holds with

$$C'_\chi = 3(C + \varepsilon).$$

For the Selesnick approximate Hilbert pairs this leads to significantly smaller constants, see Table 2, but since this does not substantially impact our the scaling of our final bounds on correlation functions we do not pursue this direction further.

4 Approximation of correlation functions

In this section we first explain how to approximate the symbols by using an approximate Hilbert pair of wavelets. We then prove our main technical result on the approximation of correlation functions.

4.1 Symbol approximations from Hilbert pairs

Recall from Eq. (2.5) that the symbol of the vacuum state of the free Dirac fermion on the real line is given by the following operator on the single-particle Hilbert space $L^2(\mathbb{R}) \otimes \mathbb{C}^2$:

$$Q = \frac{1}{2}\begin{pmatrix} \mathbb{1} & \mathcal{H} \\ -\mathcal{H} & \mathbb{1} \end{pmatrix} = \begin{pmatrix} \mathbb{1} & 0 \\ 0 & \mathcal{H}^\dagger \end{pmatrix}\left(\mathbb{1}_{L^2(\mathbb{R})} \otimes |+\rangle\langle+|\right)\begin{pmatrix} \mathbb{1} & 0 \\ 0 & \mathcal{H} \end{pmatrix}, \tag{4.1}$$

where $|+\rangle = \frac{1}{\sqrt{2}}(|0\rangle + |1\rangle)$.

To obtain a suitable approximation, consider an approximate Hilbert pair as in Definition 3.4. As before, we denote by g_w, h_w, g_s, h_s the wavelet and scaling filters, by α_j^g and α_j^h discretization maps (defined as in Eq. (3.9)) and by $W_g^{(\mathcal{L})}$ and $W_h^{(\mathcal{L})}$ the $\mathcal{L}$-layer discrete wavelet transformats (defined in Eq. (3.11)). We now approximate Eq. (4.1) by first truncating to a finite number of scales, using one of the two wavelet transforms, and then by replacing the Hilbert transform of the one wavelet basis by the other wavelet basis. Schematically,

$$\mathbb{1}_{L^2(\mathbb{R})} \rightsquigarrow \alpha_j^{h,\dagger} W_h^{(\mathcal{L}),\dagger} P_w W_h^{(\mathcal{L})} \alpha_j^h, \qquad P_w W_h^{(\mathcal{L})} \alpha_j^h \mathcal{H} \rightsquigarrow P_w W_g^{(\mathcal{L})} \alpha_j^g,$$

where $P_w = \mathbb{1}_{\ell^2(\mathbb{Z})} \otimes \sum_{k=0}^{\mathcal{L}-1} |k\rangle\langle k|$ denotes the orthogonal projection onto the wavelet coefficients.

Definition 4.1 (Approximate symbol)**.** For any approximate Hilbert pair, $j \in \mathbb{Z}$, and $\mathcal{L} \in \mathbb{N}$, define the *approximate symbol* as the following projection on $L^2(\mathbb{R}) \otimes \mathbb{C}^2$:

$$\tilde{Q}_{j,\mathcal{L}} := \alpha_j^\dagger W^{(\mathcal{L}),\dagger}\left(P_w \otimes |+\rangle\langle+|\right) W^{(\mathcal{L})} \alpha_j, \tag{4.2}$$

where $\alpha_j := \alpha_j^h \oplus \alpha_j^g$ and $W^{(\mathcal{L})} := W_h^{(\mathcal{L})} \oplus W_g^{(\mathcal{L})}$.

The symbol $\tilde{Q}_{j,\mathcal{L}}$ should be seen as an approximation of the true symbol at scales ranging from 2^{-j+1} to $2^{-j+\mathcal{L}}$.

On the circle $\mathbb{S}^1$ we proceed similarly, except that there is now a natural largest scale. For periodic boundary conditions, we use the following symbol, which intuitively approximates the true symbol at scales above $2^{-\mathcal{L}}$:

Definition 4.2 (Approximate symbol, periodic case)**.** For any approximate Hilbert pair and $\mathcal{L} \in \mathbb{N}$, define the *approximate periodic symbol* as the following projection on $L^2(\mathbb{S}^1) \otimes \mathbb{C}^2$:

$$\tilde{Q}_{\mathcal{L}}^{\mathrm{per}} := \alpha_{\mathcal{L}}^{\mathrm{per},\dagger} W^{(\mathcal{L}),\mathrm{per},\dagger}\big(P_w \otimes |+\rangle\langle +| + P_s \otimes |L\rangle\langle L|\big) W^{(\mathcal{L}),\mathrm{per}} \alpha_{\mathcal{L}}^{\mathrm{per}}, \tag{4.3}$$

where $\alpha_j^{\mathrm{per}} := \alpha_j^{h,\mathrm{per}} \oplus \alpha_j^{g,\mathrm{per}}$ and $W^{(\mathcal{L}),\mathrm{per}} := W_h^{(\mathcal{L}),\mathrm{per}} \oplus W_g^{(\mathcal{L}),\mathrm{per}}$ refer to the periodic versions as defined in Section 3.3; P_s projects onto the single scaling coefficient and $|L\rangle := \frac{1}{\sqrt{2}}(|0\rangle - i|1\rangle)$ to ensure compatibility with our choice for the Hilbert transform on constant functions.

In Section 5.3 we explain how to deal with anti-periodic boundary conditions.

Lemma 4.3. *The following relation holds:* $\alpha_j^g m(\lambda_{s,j})^\dagger \mathcal{H} = m(\mu_w)\alpha_j^g$*. Similarly, in the periodic case it holds for all* $f \in L^2(\mathbb{S}^1)$ *with zero mean that* $\alpha_j^{g,\mathrm{per}} m(\lambda_{s,j}^{\mathrm{per}})^\dagger \mathcal{H} f = m(\mu_{w,j}^{\mathrm{per}})\alpha_j^{g,\mathrm{per}} f$*.*

Proof. We want to show that $\alpha_j^g(m(\lambda_{s,j})^\dagger \mathcal{H} f) = m(\mu_w)\alpha_j^g(f)$ for $f \in L^2(\mathbb{R})$. By rescaling f it is easy to see that it suffices to show the result for $j = 0$. We know that by Eq. (3.16), $\mathcal{H} = m(\lambda_s)m(\mu_w)$, so $\alpha_0^g(m(\lambda_s)^\dagger \mathcal{H} f) = \alpha_0^g(m(\mu_w)f)$. Next we take a Fourier transform and observe that

$$\widehat{\alpha_0^g(f)}(\theta) = \frac{1}{2\pi}\sum_{n\in\mathbb{Z}} \overline{\hat{\phi}^g(\theta + 2\pi n)}\hat{f}(\theta + 2\pi n).$$

Since μ_w is 2π-periodic the result follows. In the periodic case it holds that

$$\widehat{\alpha_j^{g,\mathrm{per}}(f)}[n] = \sum_{m\in\mathbb{Z}} \overline{\hat{\phi}^{g,\mathrm{per}}[n + 2^j m]}\hat{f}[n + 2^j m].$$

which similarly implies the desired result. Note that the ambiguity in our choice of $\mathrm{sgn}(0)$ in the definition of $\mathcal{H}$ is not relevant if we assume that f has mean zero. □

The following result shows that the symbols in Eqs. (4.2) and (4.3) indeed yield reasonable approximations when restricted to appropriate functions.

Proposition 4.4. *Consider an* ε*-approximate Hilbert pair with scaling filters supported in* $\{0, \dots, M-1\}$*.*

(i) Let $f \in H^1(\mathbb{R}) \otimes \mathbb{C}^2$ *with compact support. Then, for all* $j \in \mathbb{Z}$*,* $\mathcal{L} \in \mathbb{N}$*, and* $\mathcal{L}' = 0, \dots, \mathcal{L}$*,*

$$\|\big(Q - \tilde{Q}_{j,\mathcal{L}}\big) f\| \leqslant 3\varepsilon\mathcal{L}'\|f\| + 2^{(j-\mathcal{L}')/2} 7\sqrt{MD(f)}B\|f\| + 2^{-j}5M^2\|f'\|,$$

where $B := \max\{\|\phi_g\|_\infty, \|\phi_h\|_\infty\}$*.*

(ii) Let $f \in H^1(\mathbb{S}^1) \otimes \mathbb{C}^2$*. Then, for all* $\mathcal{L} \in \mathbb{N}$ *and* $\mathcal{L}' = 0, \dots, \mathcal{L}$*,*

$$\|\big(Q^{\mathrm{per}} - \tilde{Q}_{\mathcal{L}}^{\mathrm{per}}\big) f\| \leqslant 2\varepsilon\mathcal{L}'\|f\| + 2^{-\mathcal{L}'} 9M^2\|f'\|.$$

In Theorem 4.5, we will describe how to choose j and $\mathcal{L}'$ optimally for a given number of layers $\mathcal{L}$.

Proof. (i) Let

$$\begin{aligned} Q_j &:= \begin{pmatrix} \mathbb{1} & 0 \\ 0 & \mathcal{H}^\dagger m(\lambda_{s,j}) \end{pmatrix} \alpha_j^\dagger \left(\mathbb{1}_{\ell^2(\mathbb{Z})} \otimes |+\rangle\langle+| \right) \alpha_j \begin{pmatrix} \mathbb{1} & 0 \\ 0 & m(\lambda_{s,j})^\dagger \mathcal{H} \end{pmatrix} \\ &= \alpha_j^\dagger \begin{pmatrix} \mathbb{1} & 0 \\ 0 & m(\mu_w)^\dagger \end{pmatrix} \left(\mathbb{1}_{\ell^2(\mathbb{Z})} \otimes |+\rangle\langle+| \right) \begin{pmatrix} \mathbb{1} & 0 \\ 0 & m(\mu_w) \end{pmatrix} \alpha_j, \end{aligned} \tag{4.4}$$

where we used Lemma 4.3. Then, using the first formula,

$$\begin{aligned} \|(Q - Q_j) f\| &\leqslant \frac{1}{2}\Big(\|(\mathbb{1} - \alpha_j^{h,\dagger}\alpha_j^h) f_1\| + \|(\mathbb{1} - m(\lambda_{s,j})\alpha_j^{g,\dagger}\alpha_j^g m(\lambda_{s,j})^\dagger)\mathcal{H} f_2\| \\ &\quad + \|(\mathbb{1} - m(\lambda_{s,j})\alpha_j^{g,\dagger}\alpha_j^h) f_1\| + \|(\mathbb{1} - \alpha_j^{h,\dagger}\alpha_j^g m(\lambda_{s,j})^\dagger)\mathcal{H} f_2\| \Big) \\ &= \frac{1}{2}\Big(\|(\mathbb{1} - P_j^h) f_1\| + \|(\mathbb{1} - P_j^g) m(\lambda_{s,j})^\dagger \mathcal{H} f_2\| \\ &\quad + \|(\mathbb{1} - m(\lambda_{s,j})\alpha_j^{g,\dagger}\alpha_j^h) f_1\| + \|(\mathbb{1} - \alpha_j^{h,\dagger}\alpha_j^g m(\lambda_{s,j})^\dagger)\mathcal{H} f_2\| \Big) \\ &\leqslant \frac{1}{2}\Big(\|(\mathbb{1} - P_j^h) f_1\| + \|(\mathbb{1} - P_j^h)\mathcal{H} f_2\| + \|(\mathbb{1} - P_j^g) m(\lambda_{s,j})^\dagger f_1\| + \|(\mathbb{1} - P_j^g) m(\lambda_{s,j})^\dagger \mathcal{H} f_2\| \\ &\quad + \|(\alpha_j^g m(\lambda_{s,j})^\dagger - \alpha_j^h) f_1\| + \|(\alpha_j^g m(\lambda_{s,j})^\dagger - \alpha_j^h)\mathcal{H} f_2\| \Big). \end{aligned}$$

The norms in the first line can be upper-bounded by using Lemma 3.1 (for the second, note that $\|(m(\lambda_{s,j})^\dagger f_i)'\| = \|f_i'\|$ for $i = 1, 2$). For the norms in the second line we use Lemma 3.7. Together, we find that

$$\begin{aligned} \|(Q - Q_j) f\| &\leqslant \frac{1}{2}\Big(2^{-j} C_{UV} \left(2\|f_1'\| + 2\|\mathcal{H} f_2'\| \right) + 2^{-j} C_\chi \left(\|f_1'\| + \|\mathcal{H} f_2'\| \right) \Big) \\ &\leqslant \frac{1}{2} 2^{-j} \left(2C_{UV} + C_\chi \right) \sqrt{2} \|f'\| \leqslant 2^{-j} 5 M^2 \|f'\| \end{aligned} \tag{4.5}$$

where we used that the Hilbert transform preserves the norm of the derivative ($\|\mathcal{H} f_2'\| = \|f_2'\|$).

Next, we define

$$Q_{j,\mathcal{L}} := \alpha_j^\dagger \begin{pmatrix} \mathbb{1} & 0 \\ 0 & m(\mu_w)^\dagger \end{pmatrix} \left(W_h^{(\mathcal{L}),\dagger} P_w W_h^{(\mathcal{L})} \otimes |+\rangle\langle+| \right) \begin{pmatrix} \mathbb{1} & 0 \\ 0 & m(\mu_w) \end{pmatrix} \alpha_j.$$

Using the second expression in Eq. (4.4), we can then split the remaining error as

$$\|(Q_j - \tilde{Q}_{j,\mathcal{L}}) f\| \leqslant \|(Q_j - Q_{j,\mathcal{L}'}) f\| + \|(Q_{j,\mathcal{L}'} - \tilde{Q}_{j,\mathcal{L}'}) f\| + \|(\tilde{Q}_{j,\mathcal{L}'} - \tilde{Q}_{j,\mathcal{L}}) f\| \tag{4.6}$$

The third term in Eq. (4.6) can be estimated using Lemma 3.3:

$$\begin{aligned} \|(\tilde{Q}_{j,\mathcal{L}'} - \tilde{Q}_{j,\mathcal{L}}) f\| &\leqslant \|\alpha_j^\dagger W^{(\mathcal{L}'),\dagger} (P_s \otimes |+\rangle\langle+|) W^{(\mathcal{L}')} \alpha_j f\| \leqslant \|P_{j-\mathcal{L}'} f\| \\ &\leqslant 2^{(j-\mathcal{L}')/2} \sqrt{M D(f)} \max\{\|\phi_g\|_\infty, \|\phi_h\|_\infty\} (\|f_1\| + \|f_2\|) \\ &\leqslant 2^{(j-\mathcal{L}')/2} \sqrt{2} \sqrt{M D(f)} B \|f\|. \end{aligned}$$

For the second term in Eq. (4.6), we use Eq. (3.18) in Lemma 3.5:

$$\|Q_{j,\mathcal{L}'} - \tilde{Q}_{j,\mathcal{L}'}\| \leqslant \|P_w (W_h^{(\mathcal{L})} m(\mu_w) - W_g^{(\mathcal{L})})\| + \|m(\mu_w)^\dagger W_h^{(\mathcal{L}),\dagger} - W_g^{(\mathcal{L}),\dagger}\| \leqslant 2\varepsilon \mathcal{L}'$$

Finally, for the first term in Eq. (4.6), we would like to apply Lemma 3.3, but we need to be careful because $m(\mu_w)$ does not preserve compact support. So we first use Eq. (3.19) in Lemma 3.5 to get rid of $m(\mu_w)$, and then apply Lemma 3.3:

$$\begin{aligned}
\|\left(Q_j - Q_{j,\mathcal{L}'}\right) f\| &= \|(P_s \otimes |+\rangle\langle+|)\, W_h^{(\mathcal{L}')} \begin{pmatrix} \mathbb{1} & 0 \\ 0 & m(\mu_w) \end{pmatrix} \alpha_j f\| \\
&\leqslant \|P_s(W_h^{(\mathcal{L}')} m(\mu_w) - W_g^{(\mathcal{L}')})\alpha_j^g f\| + \|(P_s \otimes \mathbb{1})\, W^{(\mathcal{L}')}\alpha_j f\| \\
&\leqslant \varepsilon_{\mathcal{L}'}\|\alpha_j^g f_2\| + 2\|P_s W_g^{(\mathcal{L}')}\alpha_j^g f\| + \|(P_s \otimes \mathbb{1})\, W^{(\mathcal{L}')}\alpha_j f\| \\
&\leqslant \varepsilon_{\mathcal{L}'}\|f\| + 3\left(\|P^g_{j-\mathcal{L}'} f_2\| + \|P^h_{j-\mathcal{L}'} f_1\|\right) \\
&\leqslant \varepsilon_{\mathcal{L}'}\|f\| + 2^{(j-\mathcal{L}')/2} 5\sqrt{M D(f)}\, B\|f\|.
\end{aligned}$$

Thus, we can upper bound Eq. (4.6) by

$$\|\left(Q_j - \tilde{Q}_{j,\mathcal{L}}\right) f\| \leqslant 3\varepsilon_{\mathcal{L}'}\|f\| + 2^{(j-\mathcal{L}')/2} 7\sqrt{M D(f)}\, B\|f\|. \tag{4.7}$$

Combining Eqs. (4.5) and (4.7) we obtain the desired bound.

(ii) Using $\phi_{0,1}^{g,\mathrm{per}} = \phi_{0,1}^{h,\mathrm{per}} = \mathbf{1}$, it is easy to see that our choice of input to the scaling layer ensures that

$$Q^{\mathrm{per}}\mathbf{1} = \tilde{Q}_{\mathcal{L}}^{\mathrm{per}}\mathbf{1},$$

so we can assume without loss of generality that f has zero mean or, equivalently, that $P_0 f = 0$ and we may apply Lemma 4.3. Similarly as before (but without having to worry about an IR cut-off), we introduce

$$Q_{\mathcal{L}}^{\mathrm{per}} := \alpha_{\mathcal{L}}^{\mathrm{per},\dagger} \begin{pmatrix} \mathbb{1} & 0 \\ 0 & m(\mu_w)^\dagger \end{pmatrix} \left(W_h^{(\mathcal{L}),\mathrm{per},\dagger} P_w W_h^{(\mathcal{L}),\mathrm{per}} \otimes |+\rangle\langle+|\right) \begin{pmatrix} \mathbb{1} & 0 \\ 0 & m(\mu_w) \end{pmatrix} \alpha_{\mathcal{L}}^{\mathrm{per}}$$

and use a triangle inequality

$$\|\left(Q^{\mathrm{per}} - \tilde{Q}_{\mathcal{L}}^{\mathrm{per}}\right) f\| \leqslant \|\left(Q^{\mathrm{per}} - Q_{\mathcal{L}'}^{\mathrm{per}}\right) f\| + \|\left(Q_{\mathcal{L}'}^{\mathrm{per}} - \tilde{Q}_{\mathcal{L}'}^{\mathrm{per}}\right) f\| + \|\left(\tilde{Q}_{\mathcal{L}'}^{\mathrm{per}} - \tilde{Q}_{\mathcal{L}}^{\mathrm{per}}\right) f\|.$$

For the first term, we use Lemmas 3.1 and 3.7 and obtain

$$\|\left(Q^{\mathrm{per}} - Q_{\mathcal{L}'}^{\mathrm{per}}\right) f\| \leqslant 2^{-\mathcal{L}'} 5M^2\|f'\|,$$

in complete analogy to Eq. (4.5). For the second term, note that we can ignore the scaling part in Eq. (4.3) since we assumed that $P_0 f = 0$. Thus, we can use Eq. (3.22) in Lemma 3.6 and find

$$\|Q_{\mathcal{L}'}^{\mathrm{per}} - \tilde{Q}_{\mathcal{L}'}^{\mathrm{per}}\| \leqslant 2\varepsilon_{\mathcal{L}'}.$$

Finally, the third term can be upper bounded by using Lemma 3.1,

$$\|\left(\tilde{Q}_{\mathcal{L}'}^{\mathrm{per}} - \tilde{Q}_{\mathcal{L}}^{\mathrm{per}}\right) f\| \leqslant \|(\mathbb{1} - P_{\mathcal{L}'}^{\mathrm{per}})f\| \leqslant 2^{-\mathcal{L}'}\sqrt{2} C_{\mathrm{UV}}\|f'\| \leqslant 2^{-\mathcal{L}'} 4M^2\|f'\|$$

(note that here we are comparing different UV cut-offs, in contrast to before). By combining these bounds we obtain the desired result. □

If we keep track of all the wavelet constants in the proof of Proposition 4.4 rather than bounding them in terms of M then the proof shows in fact the bound

$$\|\left(Q - \tilde{Q}_{j,\mathcal{L}}\right) f\| \leqslant 3\varepsilon_{\mathcal{L}'}\|f\| + 2^{(j-\mathcal{L}')/2} 7\sqrt{D(f)}\, C_{\mathrm{IR}}\|f\| + 2^{-j}\frac{1}{\sqrt{2}}(2C_{\mathrm{UV}} + C_\chi)\|f'\|, \tag{4.8}$$

which will be useful if we want to investigate numerically how fast our error bounds converge.

4.2 Approximation bounds for correlation functions

The bounds on the approximate symbol from Proposition 4.4 can be used to estimate the approximation error for correlation functions. We start with the Dirac fermion on the line, whose vacuum state is the quasi-free state ω_Q with symbol Q defined in Eq. (2.5). We are interested in correlation functions of the form involving the smeared Dirac field $\Psi(f)$ and normal-ordered quadratic operators. In the Fock representation, the two-component Dirac field is implemented by the operators $\Psi(f) := a_Q(f)$, defined as in Eq. (2.1), and the normal-ordered quadratic operators the $d\Gamma_Q(A)$ defined in Section 2.2. Thus, we wish to approximate correlation functions of the form

$$G(\{O_i\}) := \langle \Omega | O_1 \cdots O_n | \Omega \rangle \,, \tag{4.9}$$

where each O_i is either a component of $\Psi(f)$ or its adjoint $\Psi^\dagger(f)$, or a normal-ordered operator $d\Gamma_Q(A)$.

We would like to approximate such correlation functions by using the symbol $\tilde{Q}_{j,\mathcal{L}}$ defined in Eq. (4.2). Thus we fix an approximate Hilbert pair, $j \in \mathbb{Z}$, and $\mathcal{L} > 0$, and consider

$$\tilde{G}_{j,\mathcal{L}}(\{O_i\}) := \langle \Omega | \tilde{O}_1 \cdots \tilde{O}_n | \Omega \rangle \,, \tag{4.10}$$

where the $\tilde{O}_i$ are obtained from the O_i by replacing $\Psi(f)$ by $\tilde{\Psi}(f) := a_{\tilde{Q}_{j,\mathcal{L}}}(P_j f)$ and $d\Gamma_Q(A)$ by $d\Gamma_{\tilde{Q}_{j,\mathcal{L}}}(P_j A P_j)$, respectively.

On the circle, we denote the corresponding correlation functions for periodic boundary conditions by $G^{\mathrm{per}}(\{O_i\})$ and $\tilde{G}^{\mathrm{per}}_{\mathcal{L}}(\{O_i\})$, respectively. They are defined in terms of the symbol Q^{per} and its approximation $\tilde{Q}^{\mathrm{per}}_{\mathcal{L}}$ defined in Eq. (4.3). We discuss anti-periodic boundary conditions in Section 5.3 below.

The following theorem is our main technical result (already stated informally in Theorem 1.1). It states that $G(\{O_i\}) \approx \tilde{G}_{j,\mathcal{L}}(\{O_i\})$ under appropriate conditions (and similarly in the periodic case).

Theorem 4.5. *Consider an ε-approximate Hilbert pair with scaling filters supported in $\{0, \ldots, M-1\}$, scaling functions bounded by B, and $\varepsilon \in (0,1)$.*

(i) Let $f_1, \ldots, f_n$ be compactly supported functions in $H^1(\mathbb{R}) \otimes \mathbb{C}^2$ and let $A_1, \ldots, A_m$ be Hilbert-Schmidt integral operators with compactly supported kernels in $H^1(\mathbb{R}^2) \otimes M_2(\mathbb{C})$, all with L^2-norm at most 1. Let $O_i = \Psi(f_i)$ or $\Psi^\dagger(f_i)$ for $i = 1, \ldots, n$ and $O_{n+i} = d\Gamma_Q(A_i)$ for $i = 1, \ldots, m$. Then we can find, for every $\mathcal{L} > 0$, a scale $j \in \mathbb{Z}$ such that

$$\left| G(\{O_i\}) - \tilde{G}_{j,\mathcal{L}}(\{O_i\}) \right| \leqslant 8^m m!(n+m) \left(\varepsilon \log_2 \frac{3C^3 D}{\varepsilon} + C\, D^{1/3} 2^{-\frac{\mathcal{L}}{3}} \right).$$

The constant $C := (\sqrt{2M}B + M^2)$ depends only on the Hilbert pair, and the constant $D := \max\{1, d(f,A) D(f,A)\}$ depends only on the smoothness and support of the smearing functions, where $d(f,A) := \max\{\|f_i'\|, \|\nabla A_i\|\}$ and $D(f,A) := \max\{D(f_i), D(A_i)\}$; ∇A_i denotes the gradient of the kernel of A_i and $D(A_i)$ denotes the side length of the smallest square supporting the kernel.

(ii) Let $f_1, \ldots, f_n$ be functions in $H^1(\mathbb{S}^1) \otimes \mathbb{C}^2$ and let $A_1, \ldots, A_m$ be Hilbert-Schmidt integral operators with kernels in $H^1(\mathbb{S}^1) \otimes M_2(\mathbb{C})$, all with L^2-norm at most 1. Then we have, for every $\mathcal{L} > 0$, that

$$\left| G^{\mathrm{per}}(\{O_i\}) - \tilde{G}^{\mathrm{per}}_{\mathcal{L}}(\{O_i\}) \right| \leqslant 8^m m!(n+m) \left(6\varepsilon \log_2 \frac{59 M^2 D}{\varepsilon} + 26 M^2 D 2^{-\mathcal{L}} \right).$$

The constant D is defined as $D := \max\{1, \|f_i'\|, \|\nabla A_i\|\}$, with ∇A_i the gradient of the kernel of A_i.

Before giving the proof, we comment on some aspects of the theorem. The main idea behind the theorem and its proof is that the approximation of the correlation functions is accurate as long as the approximation to the symbol is accurate on the scales at which the system is probed. Quite intuitively, large support requires us to accurately approximate large scales, and strong fluctuations (large derivatives) require accuracy at small scales. The constant $D = \max\{1, d(f, A)D(f, A)\}$ reflects the number of scales needed for accurate approximation for given smearing functions f_i and kernels A_i. Intuitively, D is invariant under dilatations, reflecting the scale invariance of the theory. On the circle $\mathbb{S}^1$, there is a natural largest scale, allowing for a slightly simpler formulation. While we state the theorem for the Dirac fermion, Proposition 4.4 readily implies a similar result for correlation functions of the Majorana fermion (Section 2.4).

Our assumptions on the operators A_i imply that they are in fact trace class. Thus, the operators $d\Gamma(A_i)$ and $d\Gamma_Q(A_i)$ can be directly defined in the CAR algebra, so we could work directly with the state ω_Q on the algebra rather than in the Fock space representation. Such an approach could improve the dependence on m of the bounds, since one can estimate $\|d\Gamma_Q(A_i)\| = \|d\Gamma(A_i) - \omega_Q(d\Gamma(A_i))\| \leqslant 2\|A_i\|_1$.

While in Theorem 4.5 we order the insertions in $G(\{O_i\})$ in a particular way, other orderings are also possible. This follows either from using the commutation relations (leading to terms depending on $A_k f_l$) or by directly adjusting the proof (leading to a change in the dependence on n and m, since in the proof we would insert the particle-number projections Π_{2k} in different places).

Finally, we note that in the proofs of both Proposition 4.4 and Theorem 4.5 we bound the wavelet parameters C_{UV}, C_{IR}, and C_χ from Lemmas 3.1, 3.3, and 3.7 in terms of the support M to arrive at simpler expressions. Sharper numerical bounds can be obtained by using C_{UV}, C_{IR}, and C_χ directly (see Table 2). If one tracks these constants throughout the proof, using Eq. (4.8) rather than Proposition 4.4, one sees that C can be taken to be

$$C = 2(4C_{UV} + C_\chi) + C_{IR}. \tag{4.11}$$

The precise numerical constants are not very important, but we can use this as in Fig. 2 to illustrate Theorem 4.5 numerically for two-point functions (using Table 2 to evaluate Eq. (4.11)). We see that, even for relatively small circuit depth, our Theorem 4.5 combined with numerical results of Table 2 yields a reasonably small upper bound on the approximation error.

Proof of Theorem 4.5. (i) We first estimate the error in the correlation functions in terms of the corresponding symbols for fixed $j \in \mathbb{Z}$ and $\mathcal{L}' \in \{0, \dots, \mathcal{L}\}$. We define $Q_- := Q$, $Q_+ := \mathbb{1} - Q$, $\tilde{Q}_- := \tilde{Q}_{j,\mathcal{L}}$, and $\tilde{Q}_+ := P_j - \tilde{Q}_{j,\mathcal{L}}$ (!). For $i = 1, \dots, n$,

$$\|O_i - \tilde{O}_i\| = \|a_Q(f_i) - a_{\tilde{Q}_{j,\mathcal{L}}}(P_j f_i)\| \leqslant \|(Q_+ - \tilde{Q}_+)f_i\| + \|(Q_- - \tilde{Q}_-)f_i\|,$$

where we used the definition of the operators $\tilde{O}_i$ described above, Eq. (2.1) and that $\tilde{Q}_{j,\mathcal{L}} P_j = P_j \tilde{Q}_{j,\mathcal{L}} = \tilde{Q}_{j,\mathcal{L}}$. By Proposition 4.4, we have the estimate

$$\|(Q_- - \tilde{Q}_-)f_i\| \leqslant 3\varepsilon\mathcal{L}'\|f_i\| + 2^{(j-\mathcal{L}')/2} 7\sqrt{MD(f_i)}B\|f_i\| + 2^{-j}5M^2\|f_i'\|.$$

Moreover, using Lemma 3.1,

$$\|(Q_+ - \tilde{Q}_+)f_i\| \leqslant \|P_j f_i - f_i\| + \|(Q_- - \tilde{Q}_-)f_i\| \leqslant 2^{-j}4M^2\|f_i'\| + \|(Q_- - \tilde{Q}_-)f_i\|.$$

Thus we find that

$$\|O_i - \tilde{O}_i\| \leqslant 6\varepsilon\mathcal{L}' + 2^{(j-\mathcal{L}')/2}14\sqrt{MD(f_i)}B + 2^{-j}14M^2\|f_i'\| \tag{4.12}$$

using $\|f_i\| \leqslant 1$. For $i = n+1, \ldots, n+m$, if we let Π_n denote the projection onto the n-particle subspace of the Fock space then by Eq. (2.4) we have the bound

$$\begin{aligned}\|\big(O_i - \tilde{O}_i\big)\,\Pi_{2k}\| &\leqslant 4(2k+2)\max_{\delta=\pm}\{\|Q_\delta A_i Q_\delta - \tilde{Q}_\delta A_i \tilde{Q}_\delta\|, \|Q_\delta A_i Q_{-\delta} - \tilde{Q}_\delta A_i \tilde{Q}_{-\delta}\|_2\}\\ &\leqslant 4(2k+2)\max_{\delta=\pm}\{\|(Q_\delta - \tilde{Q}_\delta)A_i\|_2 + \|A_i(Q_\delta - \tilde{Q}_\delta)\|_2\}.\end{aligned}$$

To estimate $\|(Q_\delta - \tilde{Q}_\delta)A_i\|_2$, let $\{e_n\}$ be an orthonormal basis of $L^2(\mathbb{R}) \otimes \mathbb{C}^2$, so

$$\begin{aligned}\|(Q_\delta - \tilde{Q}_\delta)A_i\|_2^2 &= \sum_n \|(Q_\delta - \tilde{Q}_\delta)A_i e_n\|^2\\ &\leqslant \sum_n \left(\left(3\varepsilon\mathcal{L}' + 2^{(j-\mathcal{L}')/2}7\sqrt{MD(A_i)}B\right)\|A_i e_n\| + 2^{-j}9M^2\|(A_i e_n)'\|\right)^2\end{aligned}$$

using Proposition 4.4 and Lemma 3.1 (for $\delta = +$) and the fact that, by our assumption on the support of the kernel of A_i, the support of $A_i e_n$ is contained in an interval of size $D(A_i)$. Since A_i has a kernel h_i in $H^1(\mathbb{R}) \otimes M_2(\mathbb{C})$, it holds that $(A_i e_n)' = (\partial_x A_i)e_n$, where $\partial_x A_i$ denotes the integral operator with kernel $\partial_x h_i$. Thus, we conclude

$$\|(Q_\delta - \tilde{Q}_\delta)A_i\|_2 \leqslant 3\varepsilon\mathcal{L}'\|A_i\|_2 + 2^{(j-\mathcal{L}')/2}7\sqrt{MD(A_i)}B\|A_i\|_2 + 2^{-j}9M^2\|\partial_x A_i\|_2.$$

Since the adjoint of an integral operator has the transposed and conjugated kernel, we obtain the same bound on $\|A_i(Q_\delta - \tilde{Q}_\delta)\|_2 = \|(Q_\delta - \tilde{Q}_\delta)A_i^\dagger\|_2$ but with $\|\partial_y A_i\|$ in place of $\|\partial_x A_i\|$, and hence

$$\|\big(O_i - \tilde{O}_i\big)\,\Pi_{2k}\| \leqslant 4(2k+2)\left(6\varepsilon\mathcal{L}' + 2^{(j-\mathcal{L}')/2}7\sqrt{MD(A_i)}B + 2^{-j}14M^2\|\nabla A_i\|_2\right) \tag{4.13}$$

using $\|A_i\|_2 = \|h_i\| \leqslant 1$, and where we have written ∇A_i for the operator which has the gradient of h_i as kernel. To estimate the error in the correlation functions, we use a telescoping sum

$$\left|G(\{O_i\}) - \tilde{G}_{j,\mathcal{L}}(\{O_i\})\right| \leqslant \sum_{i=1}^{n+m}\delta_i, \tag{4.14}$$

where

$$\delta_i = |\langle\Omega|O_1 \cdots O_{i-1}(O_i - \tilde{O}_i)\tilde{O}_{i+1}\cdots\tilde{O}_{n+m}|\Omega\rangle|.$$

Now, $\|O_i\| \leqslant 1$ for $i = 1, \ldots, n$ by $\|f_i\| \leqslant 1$. For $i = 1, \ldots, m$, we can replace O_{n+i} by $O_{n+i}\Pi_{2(m-i)}$, and similarly for $\tilde{O}_{n+i}$. Since $\|O_{n+i}\Pi_{2(m-i)}\| \leqslant 8(m-i+1)$ by Eq. (2.3) and $\|A_{n+i}\|_2 \leqslant 1$, we find that, for $i = 1, \ldots, n$,

$$\delta_i \leqslant 8^m m!\left(6\varepsilon\mathcal{L}' + 2^{(j-\mathcal{L}')/2}14\sqrt{MD(f_i)}B + 2^{-j}14M^2\|f_i'\|\right)$$

by Eq. (4.12) and, for $i = 1, \dots, m$,

$$\delta_{n+i} \leqslant 8^m m! \left(6\varepsilon\mathcal{L}' + 2^{(j-\mathcal{L}')/2} 14\sqrt{MD(A_i)}B + 2^{-j} 14M^2\|\nabla A_i\|\right)$$

by Eq. (4.13). If we plug these bounds into Eq. (4.14) we obtain

$$\begin{aligned} &\left|G(\{O_i\}) - \tilde{G}_{j,\mathcal{L}}(\{O_i\})\right| \\ &\leqslant 8^m m!(n+m) \left(6\varepsilon\mathcal{L}' + 2^{(j-\mathcal{L}')/2} 14\sqrt{MD(f,A)}B + 2^{-j} 14M^2 d(f,A)\right), \end{aligned} \tag{4.15}$$

where we used the definitions of $D(f,A)$ and $d(f,A)$. We have thus obtained a bound on the approximation error which holds for all $j \in \mathbb{Z}$ and $\mathcal{L}' = 0, \dots, \mathcal{L}$.

We now choose j and $\mathcal{L}'$ to obtain that vanishes as the number of layers $\mathcal{L}$ increases and ε goes to zero. We first choose $j = \lceil \frac{\mathcal{L}'}{3} + \frac{1}{3}\log_2 \frac{d(f,A)^2}{D(f,A)} \rceil$ and obtain

$$\begin{aligned} \left|G(\{O_i\}) - \tilde{G}_{j,\mathcal{L}}(\{O_i\})\right| &\leqslant 8^m m!(n+m) \left(6\varepsilon\mathcal{L}' + 14(\sqrt{2M}B + M^2) d(f,A)^{1/3} D(f,A)^{1/3} 2^{-\frac{\mathcal{L}'}{3}}\right) \\ &= 8^m m!(n+m) \left(6\varepsilon\mathcal{L}' + C\, D^{1/3} 2^{-\frac{\mathcal{L}'}{3}}\right), \end{aligned}$$

using the definitions of C and D. We now choose $\mathcal{L}' = \min\{\mathcal{L}, \lceil \log_2(C^3 D/\varepsilon)\rceil\}$, which is always nonnegative, and obtain

$$\begin{aligned} \left|G(\{O_i\}) - \tilde{G}_{j,\mathcal{L}}(\{O_i\})\right| &\leqslant 8^m m!(n+m) \left(6\varepsilon \left(\log_2 \frac{C^3 D}{\varepsilon} + 1\right) + \max\{C\, D^{1/3} 2^{-\frac{\mathcal{L}}{3}}, \varepsilon\}\right) \\ &\leqslant 8^m m!(n+m) \left(6\varepsilon \log_2 \frac{3C^3 D}{\varepsilon} + C\, D^{1/3} 2^{-\frac{\mathcal{L}}{3}}\right), \end{aligned}$$

which proves the desired bound.

(ii) The proof for the circle goes along the same lines using the corresponding bound from Proposition 4.4 and $j = \mathcal{L}$. Instead of Eqs. (4.12) and (4.13), we find that, for all $\mathcal{L}' \in \{0, \dots, \mathcal{L}\}$ and for $i = 1, \dots, n$,

$$\|O_i - \tilde{O}_i\| \leqslant 4\varepsilon\mathcal{L}' + 2^{-\mathcal{L}'} 18M^2\|f_i'\| + 2^{-\mathcal{L}} 4M^2\|f_i'\| \leqslant 4\varepsilon\mathcal{L}' + 2^{-\mathcal{L}'} 22M^2\|f_i'\|,$$

while for $i = n+1, \dots n+m$,

$$\|(O_i - \tilde{O}_i)\,\Pi_{2k}\| \leqslant 8(2k+2) \left(6\varepsilon\mathcal{L}' + 2^{-\mathcal{L}'} 26M^2\|\nabla A_i\|\right).$$

Thus we obtain

$$\left|G^{\mathrm{per}}(\{O_i\}) - \tilde{G}^{\mathrm{per}}_{j,\mathcal{L}}(\{O_i\})\right| \leqslant 8^m m!(n+m) \left(6\varepsilon\mathcal{L}' + 26M^2 D 2^{-\mathcal{L}'}\right)$$

in place of Eq. (4.15). Finally, we choose $\mathcal{L}' = \min\{\mathcal{L}, \lceil \log_2 \frac{26M^2 D}{\varepsilon}\rceil\}$, which is always nonnegative, and arrive at

$$\left|G^{\mathrm{per}}(\{O_i\}) - \tilde{G}^{\mathrm{per}}_{\mathcal{L}}(\{O_i\})\right| \leqslant 8^m m!(n+m) \left(6\varepsilon \log_2 \frac{59M^2 D}{\varepsilon} + 26M^2 D 2^{-\mathcal{L}}\right).$$

This is the desired bound. □

To illustrate Theorem 4.5 and to show that the class of operators considered is an interesting class, we now describe how to compute correlation functions involving smeared stress-energy tensors. The stress-energy tensor is a fundamental object in conformal field theory. Its mode decomposition form two copies of the Virasoro algebra, encoding the conformal symmetry of the theory [28]. It is convenient to choose a different basis and write the Dirac action in the form

$$S(\Psi) = \frac{1}{2}\int \Psi^\dagger \begin{pmatrix} \overline{\partial} & 0 \\ 0 & \partial \end{pmatrix} \Psi dx dt$$

where $\partial = \partial_x + \partial_t$ and $\overline{\partial} = \partial_x - \partial_t$. Then, formally, the holomorphic component $T = T_{zz}$ of the stress-energy tensor, is the normal ordering of $\Psi_1^\dagger \partial \Psi_1$. Solutions of the Dirac equation in this basis are of the form $\chi(x,t) = \chi_+(x+t) \oplus \chi_-(x-t)$. The *unsmeared* stress energy tensor $T(x)$ (which is only a formal expression in the algebraic formalism) is given by $T(x) = d\Gamma_Q(D_x)$ where

$$D_x \begin{pmatrix} f_1 \\ f_2 \end{pmatrix} = \begin{pmatrix} \delta_x f_1' \\ 0 \end{pmatrix}$$

where δ_x is a δ-function centered at x. To smear this operator, consider two smearing functions h_x and h_t. The h_t should be thought of as a smearing in the time direction and we use the Dirac equation to interpret this on our Hilbert space corresponding to $t = 0$. Thus, we define

$$D(h) \begin{pmatrix} f_1 \\ f_2 \end{pmatrix} = \begin{pmatrix} h_x (h_t \star f_1)' \\ 0 \end{pmatrix}$$

where $\star$ denotes convolution. We then define the *smeared* stress-energy tensor by the normal-ordered second quantization: $T(h) = d\Gamma_Q(D(h))$. If h_x and h_t are compactly supported functions in $H^1(\mathbb{R})$, then the operator $T(h)$ satisfies the conditions of Theorem 4.5. In Fig. 3, (b) we show the numerical result of computing two-point functions $\langle T(h_1)T(h_2)\rangle$ using our quantum circuits, where the h_i are taken to be Gaussian smearing functions. In agreement with our theorem, we find that the two-point functions are approximated accurately for approximate Hilbert pairs of suitably good quality. (Strictly speaking, the Gaussians need to be approximated by compactly supported functions so that Theorem 4.5 applies.)

5 Quantum circuits for correlation functions

We now explain how the mathematical approximation theorem can be used to construct unitary quantum circuits (in fact, tensor networks of MERA type) that rigorously compute correlation functions for free Dirac and Majorana fermions. Finally, we discuss how symmetries are approximately implemented by our circuits.

5.1 Discrete wavelet transform and single-particle circuits

First, we describe how discrete wavelet transforms can be written as *single-particle* ('first quantized' or 'classical') linear circuits. In this context, 'single-particle' means that the state space is a direct sum of local state spaces (such as $\ell^2(\mathbb{Z}) = \bigoplus_{n\in\mathbb{Z}} \mathbb{C}$). Thus let W: $\ell^2(\mathbb{Z}) \to \ell^2(\mathbb{C}^2)$ denote a single

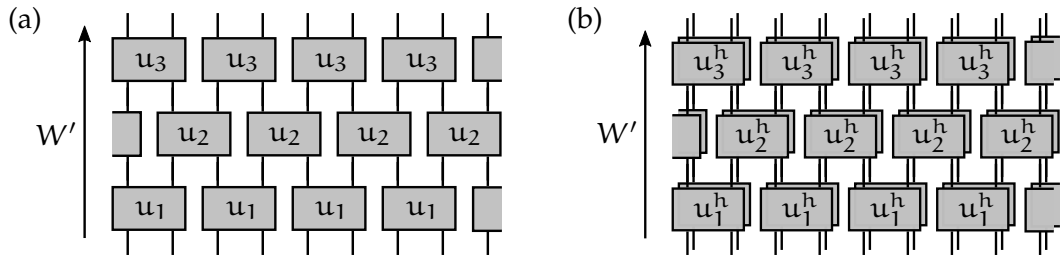

Figure 6: (a) Decomposition of the single-layer discrete wavelet transform W as a 2-local single-particle linear circuit, where we abbreviate $u_k := u(\theta_k)$. (b) Circuit for a pair of wavelet transforms, $W = W_g \oplus W_h$, where we show $u_k^h := u(\theta_k^h)$ on top of $u_k^g := u(\theta_k^g)$.

layer of a discrete wavelet transform, defined as in Eq. (3.10). By putting the scaling and wavelet outputs on the even and odd sublattice, respectively, we obtain a unitary

$$W' \colon \ell^2(\mathbb{Z}) \to \ell^2(\mathbb{Z}), \quad W' := \iota W,$$

where

$$\begin{aligned} &\iota \colon \ell^2(\mathbb{Z}) \otimes \mathbb{C}^2 \to \ell^2(\mathbb{Z}) \\ &\iota(f_w \oplus f_s)[2n] = f_w[n], \\ &\iota(f_w \oplus f_s)[2n+1] = f_s[n]. \end{aligned}$$

It has been shown in [27] that if the scaling filters are real and have length M then W' can be decomposed into a product $W' = W_{M/2} \cdots W_1$, where each $W_k : \ell^2(\mathbb{Z}) \to \ell^2(\mathbb{Z})$ is a block-diagonal unitary of the form

$$W_k = \begin{cases} \bigoplus_{r \text{ odd}} u_{r,r+1}(\theta_k) & \text{if } k \text{ odd}, \\ \bigoplus_{r \text{ even}} u_{r,r+1}(\theta_k) & \text{if } k \text{ even}. \end{cases}$$

Here, the θ_k are suitable angles and $u_{r,r+1}(\theta_k)$ denotes the unitary which acts on $\ell^2(\{r, r+1\}) \subseteq \ell^2(\mathbb{Z})$ by the rotation matrix

$$u(\theta_k) = \begin{pmatrix} \cos(\theta_k) & \sin(\theta_k) \\ -\sin(\theta_k) & \cos(\theta_k) \end{pmatrix}.$$

See [27] for a proof and for an algorithm that finds the θ_k from the filter coefficients. Thus, we obtain a decomposition of W^g into a single-particle linear circuit composed of 2-local unitaries (see Fig. 6, (a)). In the same way we can implement $\mathcal{L}$ layers of the discrete wavelet transform. Given a 2-local circuit for a wavelet transform, it is not hard to see that the periodized version of this circuit will give the periodized version of the wavelet transform. That is, the circuit has the structure shown in Fig. 1, (c), with exactly the same angles as for the original circuit on $\mathbb{Z}$ for all scales larger than zero.

Given an approximate Hilbert pair (or any pair of wavelets) we can consider $W := W_h \oplus W_g$, corresponding to performing both discrete wavelet transforms in parallel. If we apply the preceding construction to both wavelet transforms W_h and W_g we obtain two circuits, one for W_h' and one

for W'_g, parametrized by angles θ^h_k and θ^g_k for $k = 1, \ldots, M/2$. These can be assembled into a single single-particle circuit for

$$W' \colon \ell^2(\mathbb{Z}) \otimes \mathbb{C}^2 \to \ell^2(\mathbb{Z}) \otimes \mathbb{C}^2, \quad W' := W'_g \oplus W'_h$$

As shown in Fig. 6, (b), we take each site to carry two degrees of freedom (corresponding to the two components of the Dirac spinor). Instead we could also arrange the two wavelet transforms on the even and odd sublattices (by conjugating with ι). It is straightforward to see that the corresponding circuit can be implemented by 2-local unitaries and swap gates.

5.2 Second quantized circuits for correlation functions

Since we seek to describe a quantum many-body state of fermions, the circuit that we will construct is naturally a *fermionic* quantum circuit that acts on a fermionic Fock space $\mathcal{F}_\wedge(\ell^2(\mathbb{Z}))$, corresponding to a chain of fermions, by local unitaries. In our case, it will be obtained by second-quantizing the single-particle circuit for the wavelet transforms described above. Such circuits (sometimes called Gaussian fermionic circuits) can be efficiently simulated classically. If one would like to implement these circuits on a quantum computer, one would have to convert the circuit to a qubit circuit. In this case, a very natural way to do so is by applying a Jordan-Wigner transform. The resulting type of (qubit) circuit is a so-called matchgate circuit [51, 52]. We refer to [12] for further discussion of fermionic circuits in the context of wavelet transforms. For a discussion of fermionic MERA in general, see [53].

In Section 4.2, we proved that its correlation functions (4.9) are well-approximated by Eq. (4.10). We now explain how the latter can be computed by a fermionic quantum circuit of MERA type. Let us first discuss the case of the free Dirac fermion on the real line in more detail. We start with the approximate symbol (4.2), omitting the isometries $\alpha^\dagger_j$, and rewrite

$$W^{(\mathcal{L}),\dagger}\big(P_w \otimes |+\rangle\langle+|\big)W^{(\mathcal{L})} = U^{(\mathcal{L}),\dagger}_{\mathrm{MERA}} P U^{(\mathcal{L})}_{\mathrm{MERA}}, \tag{5.1}$$

where $P := P_w \otimes |0\rangle\langle 0|$ is a symbol on $\ell^2(\mathbb{Z}) \otimes \mathbb{C}^{\mathcal{L}+1} \otimes \mathbb{C}^2$ and $U^{(\mathcal{L})}_{\mathrm{MERA}} \colon \ell^2(\mathbb{Z}) \otimes \mathbb{C}^2 \to \ell^2(\mathbb{Z}) \otimes \mathbb{C}^{\mathcal{L}+1} \otimes \mathbb{C}^2$ is the unitary defined by

$$\begin{aligned} U^{(\mathcal{L})}_{\mathrm{MERA}} &:= (\mathbb{1}_{\ell^2(\mathbb{Z}) \otimes \mathbb{C}^{\mathcal{L}-1} \otimes \mathbb{C}^2} \oplus U_{\mathrm{MERA}}) \cdots (\mathbb{1}_{\ell^2(\mathbb{Z}) \otimes \mathbb{C}^2} \oplus U_{\mathrm{MERA}}) U_{\mathrm{MERA}}, \\ U_{\mathrm{MERA}} &:= (\mathbb{1}_{\ell^2(\mathbb{Z})} \otimes h) \oplus (\mathbb{1}_{\ell^2(\mathbb{Z})} \otimes \mathbb{1}_{\mathbb{C}^2}) W, \end{aligned}$$

where h is the Hadamard matrix $h = \frac{1}{\sqrt{2}}\left(\begin{smallmatrix} 1 & 1 \\ 1 & -1 \end{smallmatrix}\right)$ which maps $h|0\rangle = |+\rangle$. Just like W, U_{MERA} can be implemented by a circuit of depth $M/2 + 1$, where M is the length of the filters, obtained by composing the circuit for W with an additional layer of Hadamard unitaries acting on the wavelet outputs (see Fig. 7). The unitary $U^{(\mathcal{L})}_{\mathrm{MERA}}$ consists of $\mathcal{L}$ such circuit layers.

The key point is that in view of Eq. (5.1) we can now compute the correlation function $\tilde{G}_{j,\mathcal{L}}(\{O_i\})$ in Eq. (4.10) as follows.

Definition 5.1 (MERA correlation functions)**.** Consider an approximate Hilbert pair with filters g, h. Given a correlation function (4.9), $j \in \mathbb{Z}$, and $\mathcal{L} \geqslant 0$, we define the corresponding *MERA correlation function* by

$$G^{\mathrm{MERA}}_{j,\mathcal{L}}(\{O_i\}) := \langle \Omega | O^{\mathrm{MERA}}_1 \cdots O^{\mathrm{MERA}}_n | \Omega \rangle, \tag{5.2}$$

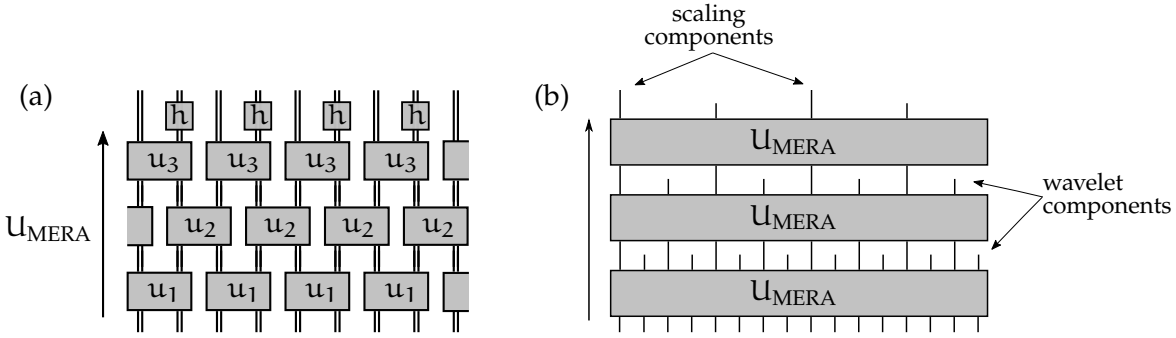

Figure 7: (a) A single MERA layer U_{MERA} before second quantization. The Hadamard unitary h (dis)entangles the modes of the two wavelet transforms that make up the Hilbert pair. We abbreviate $u_k := u_k^h \oplus u_k^g$ (cf. Fig. 6, (b)). (b) Illustration of the unitary $U_{\mathrm{MERA}}^{(\mathcal{L})}$ corresponding to $\mathcal{L}$ MERA layers before second quantization. Each layer is a local circuit of depth $M/2+1$, as in (a).

where O_i^{MERA} is obtained from O_i by replacing $\Psi(f)$ by $\Psi_{\mathrm{MERA}}(f) := a_P(U_{\mathrm{MERA}}^{(\mathcal{L})}\alpha_j f)$ and $d\Gamma_Q(A)$ by $d\Gamma_{\mathrm{MERA}}(A) := d\Gamma_P(U_{\mathrm{MERA}}^{(\mathcal{L})}\alpha_j A \alpha_j^\dagger U_{\mathrm{MERA}}^{(\mathcal{L}),\dagger})$. Here, $P := P_w \otimes |0\rangle\langle 0|$.

Importantly, P is the symbol of a state for which correlation functions can be straightforwardly evaluated. Indeed, we can intuitively think of $P = P_w \otimes |0\rangle\langle 0|$ as the symbol of a 'Fermi sea' where half of the wavelet modes are occupied (equivalently, after a Jordan-Wigner transformation this state corresponds to an 'infinite product state' where the wavelet qubits are in state $|101010\ldots\rangle$ and the scaling qubits in $|0000\ldots\rangle$). More precisely, using Eq. (2.1), we find that

$$\Psi_{\mathrm{MERA}}(f) = a_0\big((\mathbb{1}-P)U_{\mathrm{MERA}}^{(\mathcal{L})}\alpha_j f\big) + a_0^\dagger\big(\overline{PU_{\mathrm{MERA}}^{(\mathcal{L})}\alpha_j f}\big), \tag{5.3}$$

where $a_0^{(\dagger)}$ are the ordinary creation and annihilation operators on Fock space. If f is a smearing function then in order to find $\Psi_{\mathrm{MERA}}(f)$ we first compute $\alpha_j f$ either by expanding the scaling basis or simply by sampling (Lemma 3.2), then we apply $\mathcal{L}$ layers of the local circuit U_{MERA} (Fig. 7), and finally we apply the projections P and $\mathbb{1}-P$. One can proceed similarly for $d\Gamma_{\mathrm{MERA}}(A)$. This shows that the correlation functions (4.10) and (5.2) can be efficiently calculated in the single-particle picture.

We now explain how to obtain a fermionic *quantum* circuit with rigorous approximation guarantees. Suppose that, as in Theorem 4.5, we wish to approximate a correlation function involving $\Psi^{(\dagger)}(f_i)$ and $d\Gamma_Q(A_i)$, where the smearing functions f_i and the kernel of A_i are compactly supported. In this case, it is easy to see that Eq. (5.2) will involve creation and annihilation operators that act only on finitely many sites $S \subseteq \mathbb{Z}$ (which can be computed from the supports as well as the parameters j, $\mathcal{L}$, and M). In this case, we can replace $\ell^2(\mathbb{Z})$ by $\ell^2(S)$, P by its restriction P_S onto $\mathbb{H}_S := \ell^2(\mathbb{Z}) \otimes \mathbb{C}^{\mathcal{L}+1} \otimes \mathbb{C}^2$, and the infinitely wide layers U_{MERA} by finitely many local unitaries. Let us denote by $|P_S\rangle$ the corresponding Slater determinant in the fermionic Fock space $\mathcal{F}_\wedge(\mathbb{H}_S)$ and by $\Gamma_0(U_{\mathrm{MERA}}^{(\mathcal{L})}) := \bigoplus_{k=0}^\infty (U_{\mathrm{MERA}}^{(\mathcal{L})})^{\wedge k}$ the second quantizations of the single-particle unitaries $U_{\mathrm{MERA}}^{(\mathcal{L})}$. Since second quantization commutes with multiplication, this can be written as a fermionic quantum circuit composed of $\mathcal{L}$ many identical layers, each of depth $M/2+1$ (which structurally looks like Fig. 7, (b)). Thus, we recognize that $|\mathrm{MERA}_{\mathcal{L}}\rangle := \Gamma_0(U_{\mathrm{MERA}}^{(\mathcal{L})})^\dagger |P_S\rangle$ is precisely the quantum state prepared by a fermionic MERA, as illustrated in Fig. 8. Moreover, we can compute the MERA

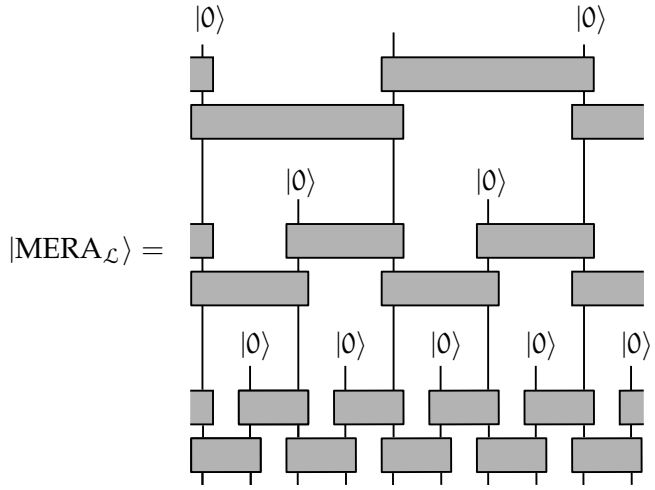

Figure 8: The MERA state is created by applying the unitary circuit to an identical product state at each level. .

correlation functions by

$$G^{\mathrm{MERA}}_{j,\mathcal{L}}(\{O_i\}) = \langle \mathrm{MERA}_{\mathcal{L}} \, |O'_1 \cdots O'_n| \, \mathrm{MERA}_{\mathcal{L}} \rangle \,, \tag{5.4}$$

where O'_i is obtained from O_i by replacing $\Psi(f)$ by $\Psi'(f) := a_0(\alpha_j f)$ and $d\Gamma_Q(A)$ by $d\Gamma_0(\alpha_j A \alpha_j^\dagger) - \langle \mathrm{MERA}_{\mathcal{L}} \, |d\Gamma_0(\alpha_j A \alpha_j^\dagger)| \, \mathrm{MERA}_{\mathcal{L}} \rangle$. Note that $\langle \mathrm{MERA}_{\mathcal{L}} \, |d\Gamma_0(\alpha_j A \alpha_j^\dagger)| \, \mathrm{MERA}_{\mathcal{L}} \rangle$ is actually *finite* because we truncated the range of wavelet scales, so this normal ordering is well-defined (even if the original operator A was not trace class). Thus, Eq. (5.4) can be interpreted as an ordinary correlation function in a fermionic MERA. This at last justifies our notation.

5.3 Circle, boundary conditions, Majorana fermions

For the circle $\mathbb{S}^1$ much the same construction applies. Given Eq. (4.3), we start with

$$W^{(\mathcal{L}),\mathrm{per},\dagger}\big(P_w \otimes |+\rangle\langle +| + P_s \otimes |L\rangle\langle L|\big) W^{(\mathcal{L}),\mathrm{per}} = U^{(\mathcal{L}),\mathrm{per},\dagger}_{\mathrm{MERA}} P_{\mathrm{per}} U^{(\mathcal{L}),\mathrm{per}}_{\mathrm{MERA}},$$

for a suitably defined unitary $U^{(\mathcal{L}),\mathrm{per}}_{\mathrm{MERA}}$ and $P_{\mathrm{per}} = P_w \otimes |0\rangle\langle 0| + P_s \otimes |L\rangle\langle L|$. This is already a symbol on a finite-dimensional Hilbert space $\mathbb{C}^{2^j} \otimes \mathbb{C}^2$. As before, $U^{(\mathcal{L}),\mathrm{per}}_{\mathrm{MERA}}$ is a product of unitaries, one for each layer, but now these unitaries will depend on the scale $j = 0, \ldots, \mathcal{L}-1$ (cf. Section 3.3). Since taking the periodization of composition of convolutions is the same as periodizing their composition, we can obtain the unitary $U^{\mathrm{per},j}_{\mathrm{MERA}}$ for the j-th layer simply by 'periodizing' the two-local unitaries U_{MERA} and analogously construct the circuit (see Fig. 1, (c)). Just like the filters, the MERA layers become identical for suffiently large j.

This leads to an approximation of the exact correlation functions $G^{\mathrm{per}}(\{O_i\})$ for periodic boundary conditions

$$G^{\mathrm{MERA,per}}_{j,\mathcal{L}}(\{O_i\}) := \langle \Omega | O^{\mathrm{MERA}}_{\mathrm{per},1} \cdots O^{\mathrm{MERA}}_{\mathrm{per},n} | \Omega \rangle \,,$$

where $O^{\mathrm{MERA}}_{\mathrm{per},i}$ is obtained from O_i by replacing $\Psi(f)$ by $\Psi^{\mathrm{per}}_{\mathrm{MERA}}(f) := a_{P_{\mathrm{per}}}(U^{(\mathcal{L}),\mathrm{per}}_{\mathrm{MERA}}\alpha^{\mathrm{per}}_j f)$ and $d\Gamma_Q(A)$ by $d\Gamma^{\mathrm{per}}_{\mathrm{MERA}}(A) := d\Gamma_{P_{\mathrm{per}}}(U^{(\mathcal{L}),\mathrm{per}}_{\mathrm{MERA}}\alpha^{\mathrm{per}}_j A\alpha^{\mathrm{per},\dagger}_j U^{(\mathcal{L}),\mathrm{per},\dagger}_{\mathrm{MERA}})$. As before, this can be interpreted as a correlation function of local operators in a fermionic MERA on a circle.

For anti-periodic boundary conditions on the circle, the symbol was given by $T^\dagger Q^{\mathrm{per}} T$ (see Section 2.3). This means that we can compute correlation functions for anti-periodic boundary conditions with the same circuit as for the periodic fermion, but replacing α_j by $\alpha_j T$. We note that the smearing functions f in this case are naturally anti-periodic (they are sections of a nontrivial bundle), so Tf is periodic and our results apply.

Finally we discuss the case of Majorana fermions. For simplicity, we only consider the case of the line (cf. Section 2.4). Suppose that we want to approximate a correlation function of the form

$$G^{\mathrm{maj}}(\{f_i\}) = \langle\Omega|\Phi(f_1)\dots\Phi(f_n)|\Omega\rangle\,, \tag{5.5}$$

where the smeared Majorana field is given by $\Phi(f) = a_0((\mathbb{1}-Q)f) + a_0^\dagger(CQf)$ in terms of the symbol Q of the free Dirac fermion, and the charge conjugation operator C defined in Eq. (2.8). Consider the self-dual CAR algebra on the range of $P' = P_w \otimes \mathbb{1}_{\mathbb{C}^2}$ which is a subspace $\mathbb{H}'$ of $\ell^2(\mathbb{Z})\otimes\mathbb{C}^2\otimes\mathbb{C}^{\mathcal{L}+1}$ (that is, the subspace corresponding to the wavelet coefficients) with charge conjugation C' given by the anti-unitary operator on $\mathbb{H}'$ which acts by $x = \left(\begin{smallmatrix}0&1\\1&0\end{smallmatrix}\right)$ in the second tensor factor and componentwise complex conjugation in the standard basis. Similarly to Eq. (5.3), define

$$\Phi^{\mathrm{MERA}}_{\mathrm{maj}}(f) = a_0\big((P'-P)U^{(\mathcal{L})}_{\mathrm{MERA}}\alpha_j f\big) + a_0^\dagger\big(C'PU^{(\mathcal{L})}_{\mathrm{MERA}}\alpha_j f\big).$$

We note that the above formula defines a representation of the self-dual CAR algebra $\mathcal{A}^{\mathrm{sd}}_\wedge(\mathbb{H}')$ since, clearly, $C'P = (P'-P)C'$. As before, we can approximate the correlation function (5.5) by

$$G^{\mathrm{MERA,maj}}_{j,\mathcal{L}}(\{f_i\}) = \langle\Omega|\Phi^{\mathrm{MERA}}_{\mathrm{maj}}(f_1)\dots\Phi^{\mathrm{MERA}}_{\mathrm{maj}}(f_n)|\Omega\rangle\,,$$

which for compactly supported f_i can be computed by an ordinary fermionic MERA. Note that

$$C'U^{(\mathcal{L})}_{\mathrm{MERA}}\alpha_j(f) = U^{(\mathcal{L})}_{\mathrm{MERA}}C\alpha_j(f) = U^{(\mathcal{L})}_{\mathrm{MERA}}\alpha_j(Cf)$$

where, with a slight abuse of notation, also write C for the similarly defined operator on $\ell^2(\mathbb{Z})\otimes\mathbb{C}^2$. Thus, we can also implement $\Gamma^c(U^{(\mathcal{L})}_{\mathrm{MERA}})$ as a circuit of Majorana fermions, mapping the state on $\mathcal{A}^{\mathrm{sd}}_\wedge(\mathbb{H}')$ corresponding to P to the state on $\mathcal{A}^{\mathrm{sd}}_\wedge(U^{(\mathcal{L})}_{\mathrm{MERA}}(\mathbb{H}'))$ with symbol $U^{(\mathcal{L}),\dagger}_{\mathrm{MERA}}PU^{(\mathcal{L})}_{\mathrm{MERA}}$.

5.4 Symmetries

For MERA tensor networks, it has been observed that the (local and global) symmetries of the underlying theory can be approximately implemented in terms of the tensor network itself [54]. In particular, a single layer of the MERA should always correspond to a rescaling by a factor two. In the wavelet construction, the relation between a single MERA layer and rescaling is very explicit.

In fact, we can show that the operator corresponding to a fermionic field has exact scaling dimension $\frac{1}{2}$, as was already observed in [12]. For this, consider (formally) the Dirac fermion field $\Psi_i(x)$, where δ_x is a delta function centered at x and $i\in\{1,2\}$. Its MERA realization at scale $j\in\mathbb{Z}$ is given by

$$\Psi^{\mathrm{MERA}}_i(x) = a^\dagger(\alpha_j(\delta_x\otimes|i\rangle)) = \sum_{k\in\mathbb{Z}}\bar\phi_{j,k}(x)a^\dagger(|k\rangle\otimes|i\rangle) \tag{5.6}$$

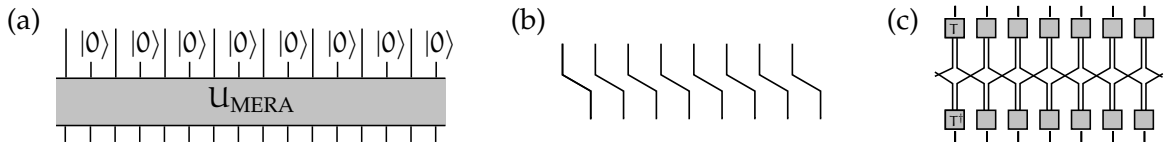

Figure 9: (a) Rescaling by a factor two is implemented by conjugation with a single MERA layer. (b) Space translation. (c) Time translation.

(we identify the CAR algebra with its representation). Since the scaling functions are compactly supported, the right-hand side expression is well-defined and we take it as the definition of $\Psi_i^{\mathrm{MERA}}(x)$. Now note that the scaling superoperator for a single MERA layer consists of a conjugation by the second quantization of U_{MERA} and a contraction with the quasi-free state with symbol $\mathbb{1}_{\ell^2(\mathbb{Z})} \otimes |+\rangle\langle +|$ on the wavelet output (cf. Fig. 9, (a)). Thus, any creation operator $a^\dagger(f)$ gets mapped to $a^\dagger(P_s W f)$, where P_s denotes the projection onto the scaling modes. Using Eq. (5.6), it follows that the scaling superoperator maps

$$\begin{aligned}
\Psi_1^{\mathrm{MERA}}(x) &\mapsto \sum_{k\in\mathbb{Z}} \bar{\phi}_{j,k}(x) a^\dagger(P_s W^h |k\rangle \otimes |1\rangle) = \sum_{k\in\mathbb{Z}} \bar{\phi}_{j,k}(x) a^\dagger((\downarrow m(\widehat{\bar{h}_s})\,|k\rangle) \otimes |1\rangle) \\
&= \sum_{k\in\mathbb{Z}} \bar{\phi}_{j,k}(x) \sum_{n\in\mathbb{Z}} \bar{h}_s[k-2n]\, a^\dagger(|n\rangle \otimes |1\rangle) = \sum_{n\in\mathbb{Z}} \bar{\phi}_{j-1,n}(x) a^\dagger(|n\rangle \otimes |1\rangle) \\
&= \sum_{n\in\mathbb{Z}} 2^{-\frac{1}{2}} \bar{\phi}_{j,n}(\frac{x}{2}) a^\dagger(|n\rangle \otimes |1\rangle) = 2^{-\frac{1}{2}}\, \Psi_1^{\mathrm{MERA}}(\tfrac{x}{2}),
\end{aligned}$$

where we used Eqs. (3.5) and (3.10). We can argue similarly for the other component, as well as for the adjoints. Thus, we conclude that a single MERA layer coarse-grains $\Psi^{\mathrm{MERA}}(x) \mapsto 2^{-\frac{1}{2}} \Psi^{\mathrm{MERA}}(\frac{x}{2})$. The interpretation is that a single layer of the MERA corresponds to a rescaling of the fields by a factor two (as it should) and that it *exactly* reproduces the correct scaling dimension of $\frac{1}{2}$ for the fermionic fields. In general the other scaling dimension of the theory are only approximately reproduced and it would be interesting to prove quantitative bounds (for example, using our Theorem 4.5).

We can also implement other global symmetries on the circuit level. Translations by steps of size 2^{-j} are trivially implemented by a circuit. Since we know the explicit time-dependence of the solutions of the Dirac equation, we can implement time translations by transforming with a basis change given by $T = \frac{1}{\sqrt{2}}\left(\begin{smallmatrix} 1 & i \\ 1 & -i \end{smallmatrix}\right)$ such that time translation shifts the first component to the right and the second component to the left. These global symmetries are shown in Fig. 9, and should be interpreted in the sense that if we want to compute correlation functions with these symmetry operators inside the correlator then we can insert the corresponding circuits. The approximation theorem and the invariance of the free fermion under these transformations show that these symmetries are indeed accurately implemented.

Acknowledgments

We acknowledge interesting discussions with Sukhbinder Singh. MW acknowledges support by the NWO through Veni grant no. 680-47-459. VBS expresses his thanks to the University of Amsterdam

and the CWI for their hospitality. He acknowledges funding by the ERC consolidator grant QUTE and thanks Frank Verstraete for discussions and his support. BGS is supported by the Simons Foundation as part of the It From Qubit Collaboration.

A Proofs of wavelet lemmas

In this section we will prove some technical lemmas involving wavelets, amongst which Lemma 3.1, Lemma 3.2, Lemma 3.3. We first state a simple Lipschitz bound for the Fourier transforms of wavelet and scaling filters.

Lemma A.1. *Let g_s be scaling filter supported in $\{0,\dots,M-1\}$. Then the corresponding wavelet filter g_w, defined in Eq.* (3.3)*, is supported in $\{2-M,\dots,1\}$ and we have that*

$$|\hat{g}_s(\theta)-\sqrt{2}| \leqslant \frac{M^2}{\sqrt{2}}\,|\theta|,$$
$$|\hat{g}_w(\theta)| \leqslant \frac{M(M+1)}{\sqrt{2}}\,|\theta|.$$

for all $\theta\in[-\pi,\pi]$.

Proof. By Eq. (3.2), $\|\hat{g}_s\|_\infty=\sqrt{2}$ and $\hat{g}_s(0)=\sqrt{2}$. Hence,

$$\|\hat{g}_s'\|_\infty \leqslant \left(\sum_{n=0}^{M-1} n\right)\|g_s\|_\infty = \frac{M(M-1)}{2}\|g_s\|_\infty \leqslant \frac{M(M-1)}{2}\|\hat{g}_s\|_\infty \leqslant \frac{M^2}{\sqrt{2}},$$

where we used that $\|f\|_\infty \leqslant \frac{1}{2\pi}\|\widehat{f}\|_1 \leqslant \|\widehat{f}\|_\infty$ for any trigonometric polynomial. Therefore,

$$|\hat{g}_s(\theta)-\sqrt{2}| \leqslant |\hat{g}_s(\theta)-\hat{g}_s(0)| \leqslant \|\hat{g}_s'\|_\infty\,|\theta| \leqslant \frac{M^2}{\sqrt{2}}\,|\theta|.$$

Now consider the corresponding wavelet filter g_w which by Eqs. (3.2) and (3.3) satisfies $\|\hat{g}_w\|_\infty=\sqrt{2}$ and $\hat{g}_w(0)=0$ and is supported in $\{2-M,\dots,1\}$. Then, similarly as above,

$$\|\hat{g}_w'\|_\infty \leqslant \left(\sum_{n=2-M}^{1} |n|\right)\|g_w\|_\infty \leqslant \frac{M(M+1)}{2}\|\hat{g}_w\|_\infty \leqslant \frac{M(M+1)}{\sqrt{2}},$$

so we obtain

$$|\hat{g}_w(\theta)| = |\hat{g}_w(\theta)-\hat{g}_w(0)| \leqslant \|\hat{g}_w'\|_\infty\,|\theta| \leqslant \frac{M(M+1)}{\sqrt{2}}\,|\theta|.$$

□

In practice, the bounds in Lemma A.1 can be pessimistic.

We now proceed to prove the lemmas in Section 3.4. Our main tool is the following technical lemma.

Lemma A.2. *Let $\chi \in H^{-K}(\mathbb{R})$ such that $\hat{\chi} \in L^\infty(\mathbb{R})$ and there exists a constant $C > 0$ such that $|\hat{\chi}(\omega)| \leqslant C|\omega|^K$ for all $|\omega| \leqslant \pi$. Define $C_\chi := (C^2 + \|\hat{\chi}\|_\infty^2/3)^{1/2}$. Then, for all $f \in H^K(\mathbb{R})$ and $j \in \mathbb{Z}$ we have that*

$$\sum_{k\in\mathbb{Z}} |\langle \chi_{j,k}, f\rangle|^2 \leqslant 2^{-2Kj} C_\chi^2 \|f^{(K)}\|^2,$$

where $\chi_{j,k}(x) := 2^{\frac{j}{2}}\chi(2^j x - k)$. Similarly, for all $f \in H^K(\mathbb{S}^1)$ and $j \geqslant 0$ we have that

$$\sum_{k=1}^{2^j} |\langle \chi_{j,k}^{\mathrm{per}}, f\rangle|^2 \leqslant 2^{-2Kj} C_\chi^2 \|f^{(K)}\|^2,$$

where $\chi_{j,k}^{\mathrm{per}}(x) = \sum_{m\in\mathbb{Z}} \chi_{j,k}(x + m)$.

Proof. For $f \in H^K(\mathbb{R})$, we start with

$$\begin{aligned}
\sum_{k\in\mathbb{Z}} \left|\langle \chi_{j,k}, f\rangle\right|^2 &= \sum_{k\in\mathbb{Z}} \left| \frac{1}{2\pi} \langle \widehat{\chi_{j,k}}, \hat{f}\rangle \right|^2 \\
&= \sum_{k\in\mathbb{Z}} \left| \frac{1}{2\pi} \int_{-\infty}^{\infty} 2^{-j/2} e^{i\omega 2^{-j}k} \overline{\hat{\chi}(2^{-j}\omega)} \hat{f}(\omega) d\omega \right|^2 \\
&= \sum_{k\in\mathbb{Z}} \left| \frac{1}{2\pi} \int_{-\infty}^{\infty} 2^{j/2} \overline{\hat{\chi}(\omega)} \hat{f}(2^j\omega) e^{i\omega k} d\omega \right|^2 . \qquad \text{(A.1)}
\end{aligned}$$

We can interpret this as the squared norm of the Fourier coefficients of the 2π-periodic function defined by

$$F(\theta) := \sum_{m\in\mathbb{Z}} 2^{j/2} \overline{\hat{\chi}(\theta + 2\pi m)} \hat{f}(2^j(\theta + 2\pi m)),$$

provided the latter is square integrable. To see this and obtain a quantitative upper bound, we note that, for every $\theta \in [-\pi, \pi]$,

$$\begin{aligned}
|F(\theta)|^2 &\leqslant 2^j \sum_{m\in\mathbb{Z}} \left| \frac{\hat{\chi}(\theta + 2\pi m)}{(\theta + 2\pi m)^K} \right|^2 \sum_{m\in\mathbb{Z}} \left| (\theta + 2\pi m)^K \hat{f}(2^j(\theta + 2\pi m)) \right|^2 \\
&= 2^{-(2K-1)j} \sum_{m\in\mathbb{Z}} \left| \frac{\hat{\chi}(\theta + 2\pi m)}{(\theta + 2\pi m)^K} \right|^2 \sum_{m\in\mathbb{Z}} \left| (2^j(\theta + 2\pi m))^K \hat{f}(2^j(\theta + 2\pi m)) \right|^2 \qquad \text{(A.2)}
\end{aligned}$$

by the Cauchy-Schwarz inequality. To bound the left-hand side series, we split off the term for $m = 0$ and use the assumptions on $\hat{\chi}$ to bound, for $|\theta| \leqslant \pi$,

$$\begin{aligned}
\sum_{m\in\mathbb{Z}} \left| \frac{\hat{\chi}(\theta + 2\pi m)}{(\theta + 2\pi m)^K} \right|^2 &= \left| \frac{\hat{\chi}(\theta)}{\theta^K} \right|^2 + \sum_{m\neq 0} \left| \frac{\hat{\chi}(\theta + 2\pi m)}{(\theta + 2\pi m)^K} \right|^2 \leqslant C^2 + \sum_{m\neq 0} \frac{|\hat{\chi}(\theta + 2\pi m)|^2}{|\theta + 2\pi m|^{2K}} \\
&\leqslant C^2 + \|\hat{\chi}\|_\infty^2 \sum_{m=1}^{\infty} \frac{2}{(\pi m)^{2K}} \leqslant C^2 + \frac{\|\hat{\chi}\|_\infty^2}{3} = C_\chi^2 \qquad \text{(A.3)}
\end{aligned}$$

If we plug this into Eq. (A.2) then we obtain

$$|F(\theta)|^2 \leqslant 2^{-(2K-1)j} C_\chi^2 \sum_{m\in\mathbb{Z}} \left|(2^j(\theta+2\pi m))^K \hat{f}(2^j(\theta+2\pi m))\right|^2$$

and hence

$$\begin{aligned}\frac{1}{2\pi}\int_{-\pi}^{\pi} |F(\theta)|^2 d\theta &\leqslant 2^{-(2K-1)j}\frac{C_\chi^2}{2\pi}\int_{-\infty}^{\infty}\left|(2^j\omega)^K\hat{f}(2^j\omega)\right|^2 d\omega \\ &= 2^{-2Kj}\frac{C_\chi^2}{2\pi}\int_{-\infty}^{\infty}\left|\omega^K\hat{f}(\omega)\right|^2 d\omega = 2^{-2Kj}C_\chi^2\|f^{(K)}\|^2,\end{aligned}$$

which is finite since $f \in H^K(\mathbb{R})$. This shows that $F \in L^2(\mathbb{R}/2\pi\mathbb{Z})$. By Parseval's theorem we can thus bound Eq. (A.1) by

$$\sum_{k\in\mathbb{Z}} \left|\langle \chi_{j,k}, f\rangle\right|^2 \leqslant 2^{-2Kj}C_\chi^2\|f^{(K)}\|^2 \leqslant 2^{-2Kj}C_\chi^2\|f^{(K)}\|^2$$

as desired.

The proof for $f \in H^K(\mathbb{S}^1)$ proceeds similarly. First note that $\widehat{g^{\mathrm{per}}}(m) = \hat{g}(2\pi m)$ if we periodize a function $g \in L^2(\mathbb{R})$ by $g^{\mathrm{per}}(x) := \sum_{n\in\mathbb{Z}} g(x+n)$, so

$$\sum_{k=1}^{2^j}\left|\langle \chi_{j,k}^{\mathrm{per}}, f\rangle\right|^2 = \sum_{k=1}^{2^j}\left|\langle \widehat{\chi_{j,k}^{\mathrm{per}}}, \hat{f}\rangle\right|^2 = \sum_{k=1}^{2^j}\left|\sum_{m\in\mathbb{Z}} 2^{-j/2} e^{i2\pi m 2^{-j}k}\overline{\hat{\chi}(2^{-j}2\pi m)}\hat{f}(m)\right|^2 \tag{A.4}$$

which we recognize as squared norm of the inverse discrete Fourier transform of a vector v with 2^j components

$$v_l := 2^{j/2}\sum_{m\in\mathbb{Z}} \overline{\hat{\chi}(2\pi m + 2\pi 2^{-j}l)}\hat{f}(2^j m + l),$$

where it is useful to take $l \in \{-2^{j-1}+1, \ldots, 2^{j-1}\}$. To see that the components of this vector are well-defined and obtain a quantitative bound, we estimate

$$\begin{aligned}|v_l|^2 &= 2^j\left|\sum_{m\in\mathbb{Z}}\overline{\hat{\chi}(2\pi m+2\pi 2^{-j}l)}\hat{f}(2^jm+l)\right|^2 \\ &\leqslant 2^j\sum_{m\in\mathbb{Z}}\left|\frac{\hat{\chi}(2\pi m+2\pi 2^{-j}l)}{(2\pi m+2\pi 2^{-j}l)^K}\right|^2\sum_{m\in\mathbb{Z}}\left|(2\pi m+2\pi 2^{-j}l)^K\hat{f}(2^jm+l)\right|^2 \\ &= 2^{-(2K-1)j}\sum_{m\in\mathbb{Z}}\left|\frac{\hat{\chi}(2\pi m+2\pi 2^{-j}l)}{(2\pi m+2\pi 2^{-j}l)^K}\right|^2\sum_{m\in\mathbb{Z}}\left|(2\pi(2^jm+l))^K\hat{f}(2^jm+l)\right|^2.\end{aligned}$$

Since $|2\pi 2^{-j}l| \leqslant \pi$, we can upper-bound the left-hand side series precisely as in Eq. (A.3),

$$|v_l|^2 \leqslant 2^{-(2K-1)j}C_\chi^2\sum_{m\in\mathbb{Z}}\left|(2\pi(2^jm+l))^K\hat{f}(2^jm+l)\right|^2,$$

and obtain

$$\|\nu\|_2^2 \leqslant 2^{-(2K-1)j} C_\chi^2 \sum_{n\in\mathbb{Z}} \left|(2\pi n)^K \hat{f}(n)\right|^2 = 2^{-(2K-1)j} C_\chi^2 \|f^{(K)}\|^2,$$

which is finite since $f \in H^K(\mathbb{S}^1)$. As before we conclude by using the Plancherel formula in Eq. (A.4) and plugging in the upper bound.

$$\sum_{k=1}^{2^j} \left|\langle \chi_{j,k}^{\mathrm{per}}, f\rangle\right|^2 = 2^{-j} \sum_{k=1}^{2^j} |\nu_k|^2 \leqslant 2^{-2Kj} C_\chi^2 \|f^{(K)}\|^2,$$

which concludes the proof. □

We next use Lemma A.2 to prove Lemma 3.1 and Lemma 3.2, which are wavelet approximation results for sufficiently smooth functions.

Proof of Lemma 3.1. For $f \in H^K(\mathbb{R})$ and $j \in \mathbb{Z}$, we have

$$\|P_j f - f\|^2 = \sum_{l>j} \sum_{k\in\mathbb{Z}} |\langle \psi_{l,k}, f\rangle|^2.$$

because the wavelets form an orthonormal basis. We would like to bound the inner series by using Lemma A.2. For this, note that since $\hat{g}_s$ is a trigonometric polynomial with a zero of order K at $\theta = \pi$, there exists a constant C such that

$$\frac{1}{\sqrt{2}}|\hat{g}_w(\theta)| = \frac{1}{\sqrt{2}}|\hat{g}_s(\theta+\pi)| \leqslant C|\theta|^K. \tag{A.5}$$

Using Eq. (3.6) and $\|\hat{\phi}\|_\infty = 1$, it follows that

$$|\hat{\psi}(\omega)| = |\frac{1}{\sqrt{2}}\hat{g}_w(\frac{\omega}{2})\hat{\phi}(\frac{\omega}{2})| \leqslant \frac{C}{2^K}|\omega|^K.$$

Since moreover $\|\hat{\psi}\|_\infty = 1$, we can invoke Lemma A.2 with $\chi = \psi$ and obtain that

$$\|P_j f - f\|^2 \leqslant \sum_{l>j} 2^{-2Kl} C_{UV}^2 \|f^{(K)}\|^2 \leqslant 2^{-2Kj} C_{UV}^2 \|f^{(K)}\|^2,$$

where $C_{UV}^2 = C^2/4^K + 1/3 \leqslant C^2 + 1/3$.

In the same way we find that, for any $f \in H^K(\mathbb{S}^1)$ and $j \geqslant 0$,

$$\|P_j^{\mathrm{per}} f - f\|^2 = \sum_{l>j} \sum_{k=1}^{2^l} |\langle \psi_{l,k}^{\mathrm{per}}, f\rangle|^2 \leqslant 2^{-2Kj} C_{UV}^2 \|f^{(K)}\|^2,$$

again by Lemma A.2.

For the last assertion, we use Lemma A.1 to see that, for $K = 1$, Eq. (A.5) always holds with $C = M(M+1)/2$, hence we have $C_{UV} \leqslant 2M^2$. □

Proof of Lemma 3.2. The trigonometric polynomial $\hat{g}_s$ satisfies $\hat{g}_s(0) = \sqrt{2}$, so there is a constant $C > 0$ such that

$$|\frac{1}{\sqrt{2}}\hat{g}_s(\theta) - 1| \leqslant C|\theta| \tag{A.6}$$

for $\theta \in [-\pi, \pi]$. Using the infinite product formula (3.8), it follows that, for all $|\omega| \leqslant \pi$,

$$|\hat{\phi}(\omega) - 1| = |\prod_{k=1}^{\infty} \frac{1}{\sqrt{2}}\hat{g}_s(2^{-k}\omega) - 1| \leqslant \sum_{k=1}^{\infty} |\frac{1}{\sqrt{2}}\hat{g}_s(2^{-k}\omega) - 1| \leqslant \sum_{k=1}^{\infty} \frac{C}{\sqrt{2}} 2^{-k}|\omega| = \frac{C}{\sqrt{2}}|\omega| \tag{A.7}$$

using a telescoping sum and the fact that $|\hat{g}_s| \leqslant \sqrt{2}$ (in fact, this holds for all $\omega \in \mathbb{R}$, but we will not need this). Now recall from Sobolev embedding theory that $\hat{f} \in L^1(\mathbb{R})$ for any $f \in H^1(\mathbb{R})$. Thus, the continuous representative of f can be computed by the inverse Fourier transform, i.e.,

$$f(x) = \frac{1}{2\pi} \int_{-\infty}^{\infty} \hat{f}(\omega) e^{i\omega x} d\omega$$

for all $x \in \mathbb{R}$. As a consequence,

$$\|\alpha_j f - f_j\|^2 = \sum_{k \in \mathbb{Z}} \left| \langle \phi_{j,k}, f \rangle - 2^{-j/2} f(2^{-j}k) \right|^2 = \sum_{k \in \mathbb{Z}} \left| \langle \chi_{j,k}, f \rangle \right|^2$$

where $\chi := \phi - \delta_0$. Now, $\hat{\chi} = \hat{\phi} - \mathbf{1}$, hence $\|\hat{\chi}\|_\infty \leqslant 2$. Together with the bound in Eq. (A.7) we obtain from Lemma A.2 that

$$\|\alpha_j f - f_j\|^2 \leqslant 2^{-2j} C_\phi \|f'\|^2,$$

where $C_\phi := C^2 + \frac{4}{3}$. The proof for $H^1(\mathbb{S}^1)$ proceeds completely analogously. Finally, Lemma A.1 shows that if the scaling filter is supported in $\{0, \dots, M-1\}$ then Eqs. (A.6) and (A.7) always hold with $C = M^2/2$. Thus, $C_\phi \leqslant 2M^2$. □

Finally, we prove Lemma 3.3, which is an approximation result for compactly supported functions.

Proof of Lemma 3.3. Let us denote by S the support of f. Since the scaling functions for fixed j form an orthonormal basis of V_j, and using Cauchy-Schwarz, we find that

$$\|P_j f\|^2 = \sum_{k \in \mathbb{Z}} |\langle \phi_{j,k}, f \rangle|^2 \leqslant \|f\|^2 \sum_{k \in \mathbb{Z}} \int_S |\phi_{j,k}(x)|^2 \, dx = \|f\|^2 \int_{2^j S} \sum_{k \in \mathbb{Z}} |\phi(y-k)|^2 \, dy.$$

This allows us to conclude that

$$\|P_j f\|^2 \leqslant \|f\|^2 2^j C_{IR}^2 D(f),$$

which confirms the claim. If ϕ is bounded and supported on an interval of width M, we can bound $\sum_{k \in \mathbb{Z}} |\phi(y-k)|^2 \leqslant M\|\phi\|_\infty^2$. □

References

[1] Román Orús. A practical introduction to tensor networks: Matrix product states and projected entangled pair states. *Annals of Physics*, 349:117–158, 2014.

[2] Jutho Haegeman, Tobias J Osborne, Henri Verschelde, and Frank Verstraete. Entanglement renormalization for quantum fields in real space. *Physical Review Letters*, 110:100402, 2013, arXiv:1102.5524.

[3] Frank Verstraete and J Ignacio Cirac. Continuous matrix product states for quantum fields. *Physical Review Letters*, 104:190405, 2010, arXiv:1002.1824.

[4] Christoph Brockt, Jutho Haegeman, David Jennings, Tobias J Osborne, and Frank Verstraete. The continuum limit of a tensor network: a path integral representation. 2012, arXiv:1210.5401.

[5] Jordan S Cotler, M Reza Mohammadi Mozaffar, Ali Mollabashi, and Ali Naseh. Entanglement renormalization for weakly interacting fields. *Physical Review D*, 99(8):085005, 2019.

[6] Jutho Haegeman, J Ignacio Cirac, Tobias J Osborne, Henri Verschelde, and Frank Verstraete. Applying the variational principle to (1+ 1)-dimensional quantum field theories. *Physical review letters*, 105(25):251601, 2010.

[7] Martin Ganahl, Julián Rincón, and Guifre Vidal. Continuous matrix product states for quantum fields: An energy minimization algorithm. *Physical review letters*, 118(22):220402, 2017.

[8] Guifré Vidal. Entanglement renormalization. *Physical Review Letter*, 99:220405, 2007, arXiv:cond-mat/0512165.

[9] Guifré Vidal. Class of quantum many-body states that can be efficiently simulated. *Physical review letters*, 101(11):110501, 2008, arXiv:quant-ph/0610099.

[10] Glen Evenbly and Guifré Vidal. Quantum criticality with the multi-scale entanglement renormalization ansatz. In *Strongly Correlated Systems*, pages 99–130. Springer, 2013, arXiv:1109.5334.

[11] Isaac H Kim and Brian Swingle. Robust entanglement renormalization on a noisy quantum computer. 2017, arXiv:1711.07500.

[12] Glen Evenbly and Steven R White. Entanglement renormalization and wavelets. *Physical Review Letter*, 116:140403, 2016, arXiv:1602.01166.

[13] Jutho Haegeman, Brian Swingle, Michael Walter, Jordan Cotler, Glen Evenbly, and Volkher B Scholz. Rigorous free-fermion entanglement renormalization from wavelet theory. *Physical Review X*, 8:011003, 2018, arXiv:1707.06243.

[14] Freek Witteveen and Michael Walter. Bosonic entanglement renormalization circuits from wavelet theory. *SciPost Phys*, 10:143, 2021.

[15] Juan Maldacena. The large-N limit of superconformal field theories and supergravity. *International Journal of Theoretical Physics*, 38:1113–1133, 1999, arXiv:hep-th/9711200.

[16] Brian Swingle. Entanglement renormalization and holography. *Physical Review D*, 86:065007, 2012, arXiv:0905.1317.

[17] Ning Bao, ChunJun Cao, Sean M Carroll, Aidan Chatwin-Davies, Nicholas Hunter-Jones, Jason Pollack, and Grant N Remmen. Consistency conditions for an AdS multiscale entanglement renormalization ansatz correspondence. *Physical Review D*, 91(12):125036, 2015.

[18] Ashley Milsted and Guifré Vidal. Geometric interpretation of the multi-scale entanglement renormalization ansatz. *arXiv preprint arXiv:1812.00529*, 2018.

[19] Fernando Pastawski, Beni Yoshida, Daniel Harlow, and John Preskill. Holographic quantum error-correcting codes: Toy models for the bulk/boundary correspondence. *Journal of High Energy Physics*, 2015:1–55, 2015, arXiv:1503.06237.

[20] Zhao Yang, Patrick Hayden, and Xiao-Liang Qi. Bidirectional holographic codes and sub-AdS locality. *Journal of High Energy Physics*, 2016:175, 2016, arXiv:1510.03784.

[21] Patrick Hayden, Sepehr Nezami, Xiao-Liang Qi, Nathaniel Thomas, Michael Walter, and Zhao Yang. Holographic duality from random tensor networks. *Journal of High Energy Physics*, 2016: 9, 2016, arXiv:1601.01694.

[22] Sepehr Nezami and Michael Walter. Multipartite entanglement in stabilizer tensor networks. 2016, arXiv:1608.02595.

[23] Guy Battle. *Wavelets and renormalization*. World Scientific, 1999.

[24] Xiao-Liang Qi. Exact holographic mapping and emergent space-time geometry. 2013, arXiv:1309.6282.

[25] Ching Hua Lee. Generalized exact holographic mapping with wavelets. *Physical Review B*, 96: 245103, 2017, arXiv:1609.06241.

[26] Sukhwinder Singh and Gavin K Brennen. Holographic construction of quantum field theory using wavelets. 2016, arXiv:1606.05068.

[27] Glen Evenbly and Steven R White. Representation and design of wavelets using unitary circuits. *Physical Review A*, 97(5):052314, 2018, arXiv:1605.07312.

[28] Philippe Francesco, Pierre Mathieu, and David Sénéchal. *Conformal Field Theory*. Springer Science & Business Media, 2012.

[29] Ivan W Selesnick. The design of approximate Hilbert transform pairs of wavelet bases. *IEEE Trans. Sig. Process.*, 50(5):1144–1152, 2002.

[30] Ivan W Selesnick, Richard G Baraniuk, and Nick C Kingsbury. The dual-tree complex wavelet transform. *IEEE signal processing magazine*, 22(6):123–151, 2005.

[31] Runyi Yu and Huseyin Ozkaramanli. Hilbert transform pairs of orthogonal wavelet bases: Necessary and sufficient conditions. *IEEE Transactions on Signal Processing*, 53(12):4723–4725, 2005.

[32] Kunal Narayan Chaudhury and Michael Unser. Construction of Hilbert transform pairs of wavelet bases and Gabor-like transforms. *IEEE Transactions on Signal Processing*, 57(9):3411–3425, 2009.

[33] Kunal Narayan Chaudhury and Michael Unser. On the Hilbert transform of wavelets. *IEEE transactions on signal processing*, 59(4):1890–1894, 2010.

[34] Sophie Achard, Irène Gannaz, Marianne Clausel, and François Roueff. New results on approximate Hilbert pairs of wavelet filters with common factors. 2017, arXiv:1710.09095.

[35] John L Cardy. Operator content of two-dimensional conformally invariant theories. *Nuclear Physics B*, 270:186–204, 1986.

[36] Robert NC Pfeifer, Glen Evenbly, and Guifré Vidal. Entanglement renormalization, scale invariance, and quantum criticality. *Physical Review A*, 79(4):040301, 2009, arXiv:0810.0580.

[37] Isaac H Kim and Michael J Kastoryano. Entanglement renormalization, quantum error correction, and bulk causality. *Journal of High Energy Physics*, 2017:40, 2017, arXiv:1701.00050.

[38] Jürgen Fuchs. *Affine Lie algebras and quantum groups: An introduction, with applications in conformal field theory*. Cambridge University Press, 1995.

[39] Antony Wassermann. Operator algebras and conformal field theory III. fusion of positive energy representations of $\mathrm{LSU}(\mathrm{N})$ using bounded operators. *Inventiones mathematicae*, 133(3): 467–538, 1998.

[40] Modjtaba Shokrian Zini and Zhenghan Wang. Conformal field theories as scaling limit of anyonic chains. *Communications in Mathematical Physics*, 363:877–953, 2018, arXiv:1706.08497.

[41] Robert König and Volkher B Scholz. Matrix product approximations to multipoint functions in two-dimensional conformal field theory. *Physical review letters*, 117(12):121601, 2016, arXiv:1601.00470.

[42] Robert König and Volkher B Scholz. Matrix product approximations to conformal field theories. *Nuclear Physics B*, 920:32–121, 2017, arXiv:1509.07414.

[43] John Preskill. Quantum computing in the NISQ era and beyond. 2018, arXiv:1801.00862.

[44] Ola Bratteli and Derek W Robinson. *Operator Algebras and Quantum Statistical Mechanics 2*. Springer, 2003.

[45] Alan Carey and Simon Ruijsenaars. On fermion gauge groups, current algebras and Kac-Moody algebras. *Acta Applicandae Mathematica*, 10:1–86, 1987.

[46] Lars-Erik Lundberg. Quasi-free "second quantization". *Communications in Mathematical Physics*, 50:103–112, 1976.

[47] Huzihiro Araki. On quasifree states of CAR and Bogoliubov automorphisms. *Publications of the Research Institute for Mathematical Sciences*, 6:385–442, 1971.

[48] Stéphane Mallat. *A Wavelet Tour of Signal Processing*. Academic Press, 2008.

[49] Przemyslaw Wojtaszczyk. *A Mathematical Introduction to Wavelets*. Cambridge University Press, 1997.

[50] Ivan W Selesnick. Hilbert transform pairs of wavelet bases. *IEEE Signal Processing Letters*, 8: 170–173, 2001.

[51] Sergey B Bravyi and Alexei Y Kitaev. Fermionic quantum computation. *Annals of Physics*, 298: 210–226, 2002, arXiv:quant-ph/0003137.

[52] Richard Jozsa and Akimasa Miyake. Matchgates and classical simulation of quantum circuits. In *Proceedings of the Royal Society of London A: Mathematical, Physical and Engineering Sciences*, volume 464, pages 3089–3106, 2008, arXiv:0804.4050.

[53] Philippe Corboz and Guifré Vidal. Fermionic multiscale entanglement renormalization ansatz. *Physical Review B*, 80:165129, 2009, arXiv:0907.3184.

[54] Ashley Milsted and Guifré Vidal. Tensor networks as conformal transformations. 2018, arXiv:1805.12524.